Global and Planetary Change 207 (2021) 103677

Contents lists available at ScienceDirect

Global and Planetary Change

journal homepage: www.elsevier.com/locate/gloplacha

Research Article

Transition between Variscan and Alpine cycles in the Pyrenean-Cantabrian Mountains (N Spain): Geodynamic evolution of near-equator European Permian basins

Joan Lloret [a,b], José López-Gómez [a,*], Nemesio Heredia [c], Fidel Martín-González [d], Raúl de la Horra [b], Violeta Borruel-Abadía [b,e], Ausonio Ronchi [f], José F. Barrenechea [a,g], Joaquín García-Sansegundo [h], Carlos Galé [i], Teresa Ubide [j], Nicola Gretter [k], José B. Diez [l], Manuel Juncal [l], Marceliano Lago [i]

[a] *Instituto de Geociencias (UCM, CSIC), C/Doctor Severo Ochoa 7, E-28040 Madrid, Spain*
[b] *Departamento de Geodinámica, Estratigrafía y, Paleontología, Facultad de Geología, Universidad Complutense de Madrid, C/José Antonio Nováis 12, E-28040 Madrid, Spain*
[c] *Instituto Geológico y Minero de España (IGME), C/Matemático Pedrayes 25, E33005 Oviedo, Spain*
[d] *Área de Geología-ESCET, Universidad Rey Juan Carlos, C/Tulipán, s/n, Móstoles, Madrid 28933, Spain*
[e] *Departamento de Geología, Facultad de Ciencias, Universidad de Salamanca, 37008 Salamanca, Spain*
[f] *Dipartimento di Scienze della Terra e dell'Ambiente, Università degli studi di Pavia, Via Ferrata 7, 27100 Pavia, Italy*
[g] *Departamento de Mineralogía y Petrología, Facultad de Geología, Universidad Complutense, C/José Antonio Nováis 2, 28040 Madrid, Spain*
[h] *Departamento de Geología, Universidad de Oviedo, C/Jesús Arias de Velasco s/n, E33005 Oviedo, Spain*
[i] *Department of Earth Sciences, University of Zaragoza, C/Pedro Cerbuna s/n, 50009 Zaragoza, Spain*
[j] *School of Earth and Environmental Sciences, The University of Queensland, Steele Building, Brisbane, QLD 4072, Australia*
[k] *Liceo "A. Rosmini", Corso Bettini 86, 38068 Rovereto, Italy*
[l] *Departamento de Xeociencias Mariñas e Ordenación do Territorio, Facultade de Ciencias do Mar, Universidade de Vigo. Campus As Lagoas - Marcosende, E-36310 Vigo, Spain*

A R T I C L E I N F O

Editor: Matenco Liviu

Keywords:
Late Carboniferous
Early Permian
Post-Variscan extension
Variscan collapse
Pangea break-up
Pyrenean-Cantabrian orogen
Late Paleozoic Ice Age

A B S T R A C T

In the northern Iberian Peninsula, the Pyrenean-Cantabrian orogenic belt extends E-W for ca. 1000 km between the Atlantic Ocean and Mediterranean Sea. This orogen developed from the collision between Iberia and Eurasia, mainly in Cenozoic times. Lower-middle Permian sediments crop out in small, elongated basins traditionally considered independent from each other due to misinterpretations on incomplete lithostratigraphic data and scarce radiometric ages. Here, we integrate detailed stratigraphic, sedimentary, tectonic, paleosol and magmatic data from well-dated lithostratigraphic units. Our data reveal a similar geodynamic evolution across the Pyrenean-Cantabrian Ranges at the end of the Variscan cycle.

Lower-middle Permian basins started their development under an extensional regime related to the end of the Variscan Belt collapse, which stars in late Carboniferous times in the Variscan hinterland. This orogenic collapse transitioned to Pangea breakup at the middle Permian times in the study region. Sedimentation occurred as three main tectono-sedimentary extensional phases. A first phase (Asselian-Sakmarian), which may have even started at the end of the Carboniferous (Gzhelian) in some sections, is mainly represented by alluvial sedimentation associated with calc-alkaline magmatism. A second stage (late Artinskian–early Kungurian), represented by alluvial, lacustrine and palustrine sediments with intercalations of calc-alkaline volcanic beds, shows a clear upward aridification trend probably related to the late Paleozoic icehouse-greenhouse transition. The third and final stage (Wordian-Capitanian) comprised of alluvial deposits with intercalations of alkaline and mafic beds, rarely deposited in the Cantabrian Mountains, and underwent significant pre- and Early Mesozoic erosion in some segments of the Pyrenees. This third stage can be related to a transition towards the Pangea Supercontinent breakup, not generalized until the Early/Middle Triassic at this latitude because the extensional process stopped about 10 Myr (Pyrenees) to 30 Myr (Cantabrian Mountains).

* Corresponding author.
E-mail address: jlopez@ucm.es (J. López-Gómez).

https://doi.org/10.1016/j.gloplacha.2021.103677
Received 24 April 2021; Received in revised form 25 September 2021; Accepted 9 October 2021
Available online 16 October 2021

When compared to other well-dated basins near the paleoequator, the tectono-sedimentary and climate evolution of lower-middle Permian basins in Western and Central Europe shows common features. Specifically, we identify coeval periods with magmatic activity, extensional tectonics, high subsidence rates and thick sedimentary record, as well as prolonged periods without sedimentation. This comparison also identifies some evolutionary differences between Permian basins that could be related to distinct locations in the hinterland or foreland of the Variscan orogen. Our data provide a better understanding of the major crustal re-equilibration and reorganization that took place near the equator in Western-Central Europe during the post-Variscan period.

1. Introduction

The Pyrenean-Cantabrian orogenic belt extends *E*-W about 1000 km in the northern Iberian Peninsula from the Mediterranean Sea to the Atlantic Ocean (Fig. 1a). The orogen was the result of Iberia-Eurasia collision (Alpine Pyrenean orogeny) and mainly developed in Cenozoic times (Muñoz, 2019 and references therein). This orogenic belt is subdivided into two mountain ranges: i) the Pyrenees to the east, forming the isthmus between Iberia and the rest of Europe, and ii) the Cantabrian Mountains to the west, extending along the northern Iberia coastline (Pulgar et al., 1996, 1999; Gallastegui et al., 2002; Barnolas and Pujalte, 2004; Pedreira et al., 2007; Martín-González and Heredia, 2011a, 2011b; Martín-González et al., 2012; Barnolas et al., 2019) (Fig. 1a). The Pyrenean-Cantabrian belt is the outcome of progressive Alpine inversion and deformation of previous Permian-Mesozoic basins in the eastern Cantabrian Mountains (Vasco-Cantábrica Region, Fig. 1a)

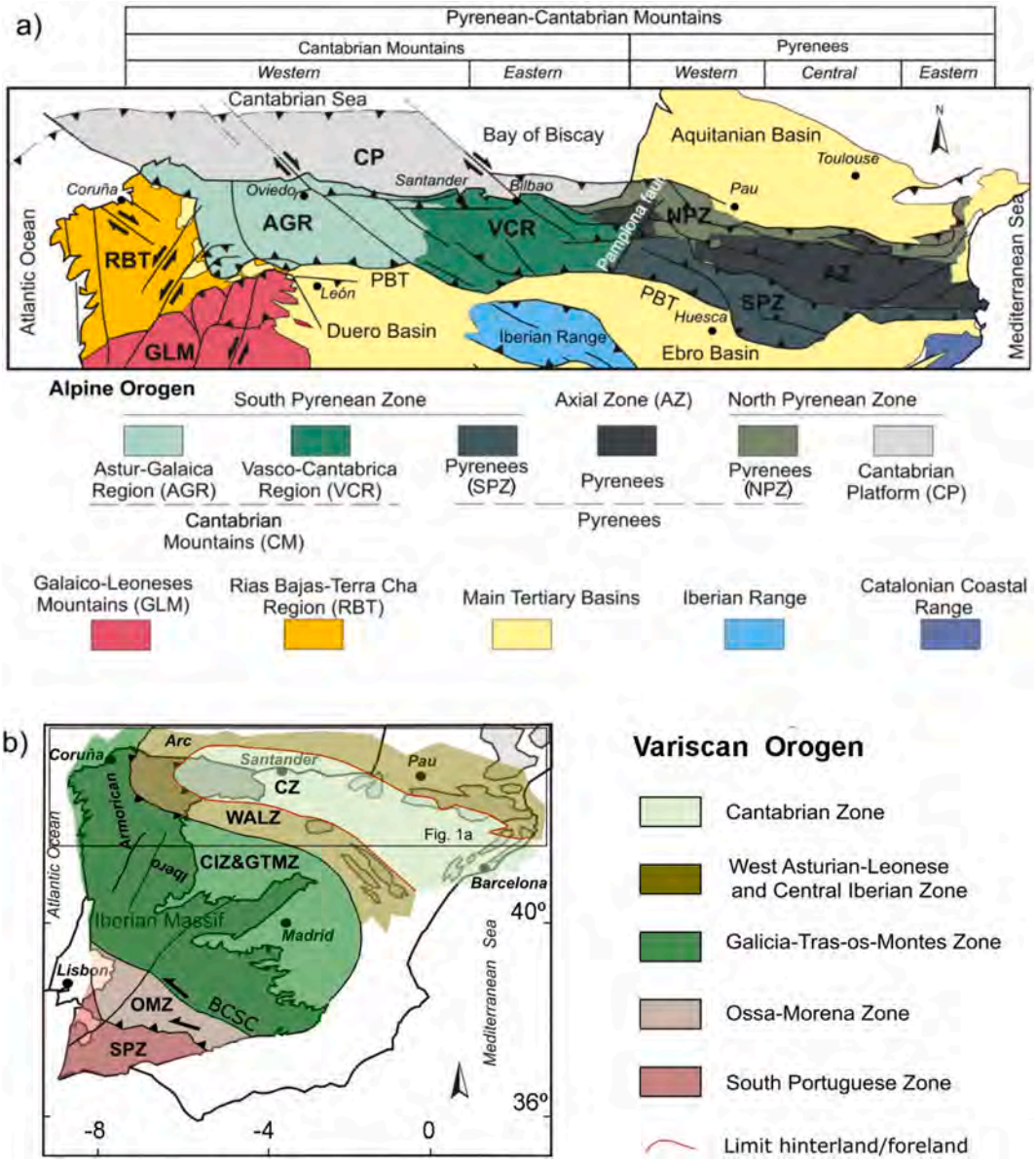

Fig. 1. a) Structural sketch showing the tectono-stratigraphic regions of the Alpine Pyrenean-Cantabrian Orogen in the north of the Iberian Peninsula (modified from Martín-González and Heredia, 2011a) and geographical subdivisions (based on Muñoz, 2002). b) Zones of the Variscan Orogen in Iberia and the Ibero-Armorica Arc (Modified from García-Sansegundo et al., 2011).

and Pyrenees (Capote et al., 2002; Barnolas and Pujalte, 2004; Pedreira et al., 2007). This was accompanied by reactivation of Variscan basement structures in the western part of the Cantabrian Mountains (Martín-González et al., 2021 and references therein) (Astur-Galaica Region, Fig. 1a, b), where the Variscan belt shows a prominent shape and the Mesozoic sediments are scarce or barely recorded (Martín-González and Heredia, 2011a, 2011b). After the end of the Variscan cycle, Permian-Mesozoic basins produced by three extensional phases characterized the pre-orogenic stage of the Alpine cycle. These extensional phases have been dated as early Permian, middle Permian–Late Triassic and Late Jurassic–Early Cretaceous, with a thermal subsidence period developed between the last two phases (Teixell, 1998; Muñoz, 2002; Capote et al., 2002; Fernández-Viejo et al., 2011; Carballo et al., 2015; Martín-Chivelet et al., 2019; López-Gómez et al., 2019a, 2019b). Subsequent Cenozoic compressive deformation, associated with the Alpine orogeny, partially overprinted the original extensional structure of the Permian-Mesozoic basins (Vergés and Burbank, 1996; Sinclair et al., 2005; Jolivet et al., 2007; Vacherat et al., 2014).

The sedimentary record that filled these initial Permian troughs included volcanic and volcaniclastic products. This volcanic activity, mostly of calc-alkaline affinity with mixed mantle and crustal sources, played an important role in the evolution of those first basins (e.g., Bixel, 1984; Lago et al., 2004a, 2004b, 2019; Galé, 2005; Maino et al., 2012; Pereira et al., 2014). Owing to the development of large Mesozoic basins and subsequent Alpine deformation, the Permian basin outcrops are very fragmented. Because of this, local studies conducted over the past decades led to the definition of numerous lithostratigraphic units across the Pyrenean-Cantabrian ranges. This has made it difficult to establish correlations and histories of the Late Paleozoic-lower Mesozoic sedimentary record as a whole. Studies focused on latest Carboniferous-early Permian rocks, or the transition from the Variscan cycle (Cambrian-early Permian) to the Alpine cycle (early Permian-early Neogene), have encountered even more difficulties, as those sedimentation stages were still linked to small isolated continental basins, and precise ages of the units are scarce. Hence, there is no clear understanding of the lateral connections of tectono-sedimentary evolution during the first sedimentation stages of the Alpine cycle in the Pyrenean-Cantabrian orogenic belt. Consequently, these basins have been considered to develop independently, with different tectonic controls and sedimentary refill in each structural region (Fig. 1a). As a whole, the early Alpine sedimentation of the Cantabrian basins has been considered independently from the rest of the Pyrenean basins (see López-Gómez et al., 2002, 2019a, 2019b and references therein). Such sedimentary evolution has also been considered independently from that of neighboring basins of the same age in Western and Central Europe, complicating broad paleogeographic reconstructions.

In contrast, the Cantabrian-Pyrenean orogen has been considered as a whole over the past 20 years (e.g., Gallastegui et al., 2002; Muñoz, 2002; Barnolas and Pujalte, 2004; Barnolas et al., 2019; López-Gómez et al., 2019b; Muñoz, 2019). New dating efforts have attempted to simplify the Mesozoic and Cenozoic stratigraphy in the different structural zones of the Pyrenean Ranges (Vergès and García Senz, 2001; Gretter et al., 2015, 2019; Carballo et al., 2015; Muñoz, 2002; López-Gómez et al., 2002, 2019b; Martín-Chivelet et al., 2002, 2019). However, the identification of events at the scale of tectonostratigraphic units across the Permian and Triassic basins in these ranges has been lacking to date.

The present study presents an updated stratigraphy with new age data obtained from paleontological and radiometric analyses, along with a detailed study of sedimentology, tectonics, paleosols and syntectonic magmatism. Our aim is to examine the transition between the Variscan and Alpine cycles (latest Carboniferous to early-middle Permian), as the Variscan orogenic collapsed and transitioned into the Pangea rift system. We apply a multi-disciplinary approach to: a) characterize igneous and sedimentary rocks and the basins that host them, b) establish if the transition between orogenic cycles involved the same tectonosedimentary pulses in the Cantabrian Ranges and the Pyrenees, c) assess if these pulses can be recognized in other contemporary basins of Western and Central Europe, d) characterize the onset, progression and ending of the Variscan orogenic collapse, leading into Pangea rifting, e) propose a new geodynamic and palaeogeograpic scenario that provides a better understanding of the latest Carboniferous-Permian basins in the context of the equatorial Variscan fold belt.

2. Geological and geodynamic setting

The cartographic continuity of the Pyrenees and Cantabrian Mountains in the northern Iberian Peninsula suggests these mountain ranges are part of a continuous Alpine orogen which trends ESE-WNW to E-W along >800 km (Choukroune et al., 1990; Pulgar et al., 1996; Teixell, 1998, Teixell et al., 2018; Muñoz, 2002; Gallastegui et al., 2002; Barnolas and Pujalte, 2004; Martín-González and Heredia, 2011a) (Fig. 2).

The Pyrenees show a double asymmetric vergence (Choukroune et al., 1990; Choukroune, 1992; Muñoz, 1992; Teixell, 1998). The South Pyrenean Zone shows thin-skinned tectonics, characterized by a south-directed fold and thrust belt, whose basal detachment used the Upper Triassic evaporites (Figs. 1a, 2). The Northern Pyrenean Zone is narrower and features thick-skinned tectonics characterized by north-directed Alpine thrusts, which deform the Paleozoic Variscan basement. Many of these thrusts are the result of reactivation of normal Mesozoic faults (Muñoz, 1992; Teixell, 1998). Between both zones, the Pyrenean Axial Zone contains Alpine south-directed thrusts, which jointly deform the Mesozoic-Cenozoic cover and Carboniferous and earlier rocks, previously deformed by the Variscan orogeny. In the Central Pyrenees, the southern part of the Axial Zone constitutes an antiformal-stack constructed by Alpine thrusts (Déramond et al., 1985; Williams and Fischer, 1984). Associated with the Alpine Pyrenean orogeny, two continental Cenozoic foreland basins develop: the Ebro Basin in the south and the Aquitaine Basin in the north, located in the orogen periphery (Choukroune et al., 1990; Muñoz, 1992) (Fig. 1a).

The Cantabrian Mountains trend *E*-O. They constitute the western extension of the Pyrenees and show a mainly south-vergent Alpine structure. The Cantabrian Mountains can be correlated with the South Pyrenean Zone (Fig. 1a), while the Ebro foreland basin continues to the west into the Duero Basin (Alonso et al., 1996). Further, the structures of the North Pyrenean Zone continue offshore into the Landes Plateau and the Cantabrian Platform of the Bay of Biscay (Fig. 1a) (Cámara, 1997; Gallastegui et al., 2002). The Cantabrian Mountains have been classified into two tectono-stratigraphic regions: the Vasco-Cantabrica Region (VCR) to the east and the Astur-Galaica Region (AGR) to the west (Martín-González and Heredia, 2011a and references therein) (Fig. 1a). According these authors, the Vasco Cantábrica Region is characterized by a thick and complete succession of Mesozoic sediments (Triassic to Cretaceous) deposited in a complex subsident extensional basin (the Basque-Cantabrian Basin). These Mesozoic sediments unconformably cover a Paleozoic Variscan basement that only crops out in the western and eastern borders of the VCR (Cabuerniga Promontory and Basque Massifs, respectively). The Astur Galaica Region is characterized by its lack or scarcity of Mesozoic sedimentary rocks, which unconformably rest on a large outcrop of the Variscan basement (Iberian Massif). Only in the eastern part, a fairly complete but no continuous sedimentary sequence of Mesozoic sediments appears (the Asturian Basin). Therefore, the Alpine deformation in the AGR mainly affects the basement of the Iberian Massif, which consists of Paleozoic rocks with Variscan compressive deformation (Late Devonian-earliest Permian) (Fig. 1b) represented by thrusts, folds and dextral strike-slip faults developed in late Variscan times.

In the Pyrenean-Cantabrian Ranges, the formation of extensional lower Permian basins during a stage of orogenic collapse (López-Gómez et al., 2021) represents the end of the Variscan orogeny and the beginning of the Alpine cycle (Martínez-García, 1981).

In the Cantabrian Mountains, lower Permian extensional basins are

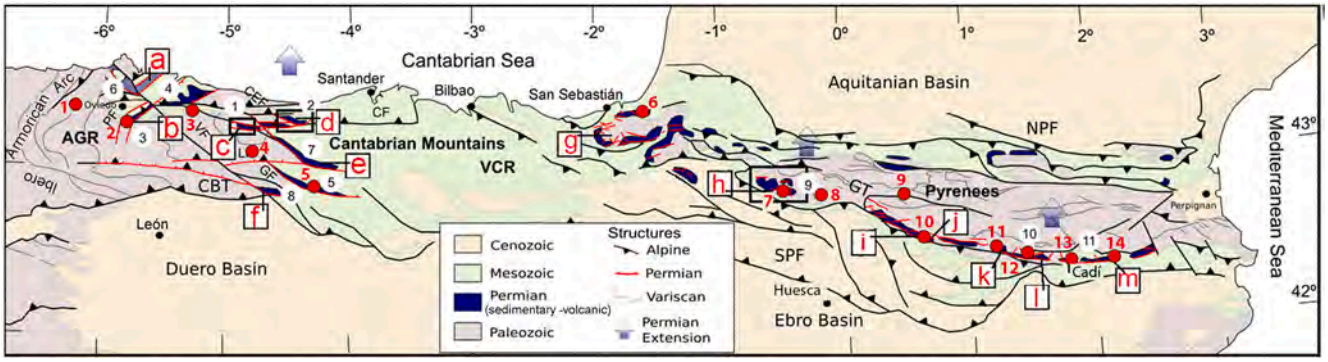

Fig. 2. Geological sketch showing the locations of the main Permian basins and faults in the present position of the Alpine Pyrenean-Cantabrian Orogen. Permian basins (numbers in white circles): 1) Sotres, 2) La Hermida-Carmona, 3) la Justa-Aramil, 4) Villaviciosa 5) Peña Labra, 6) Villabona, 7) Peña Sagra, 8) Rueda, 9) Somport-Anayet, 10) Estac-Baró, and 11) Castellar de N'Hug. Main faults (letters in White squares): VF- Ventaniella Fault, CF- Cabuerniga Fault, CEF- Celis Fault, GF- Golobar Fault, LF- Liebana Fault, PF- La Peña Fault, NPF- North Pyrenean Fault, SPF- South Pyrenean front, GT- Gavarnie thrust, and CBT- Cantabrian basal thrust. Arrows indicate the direction of extension during Permian times. Faults or fault segments active during the Permian are shown in red. Sections: a) La Camocha (borehole), b) Acebal-Siero, c) Sotres-Tresviso, d) Carmona, e) Peña Sagra, f) Rueda, g) Maya, h) Aragón-Bearn, i) Castejón-Laspaúles, j) Gotarta, k) Malpás-Erill Castell, l) Baró-Estac, and m) Castellar de N'Hug. Numbers in red circles indicate the location of the studied magmatisms.

elongated, narrow and isolated, although some of these appear close to each other and may be interconnected (López-Gómez et al., 2019a). These basins, unlike in the Pyrenees, contain only lower Permian (Cisuralian) rocks that unconformably rest over Carboniferous sediments deposited in the most external zone of the Variscan orogen, the Cantabrian Zone (Fig. 1a, b). The general structure of this zone is an arc-shaped thrust and fold belt (Julivert, 1971; Julivert and Marcos, 1973; Pérez-Estaún et al., 1988), named Asturian Arc or Ibero-Armorican Arc (Fig. 1b). In the westernmost sectors of the Cantabrian Zone, the Kasimovian-Gzhelian (late Carboniferous) sedimentary record is continental and mainly post-tectonic. However, in the eastern part, corresponding to the outermost sectors of the Variscan foreland, the sedimentary record of this same age is syntectonic and still of marine origin (Rodríguez-Fernández and Heredia, 1987; Merino-Tomé et al., 2009, 2017). At the Carboniferous-Permian boundary (late Gzhelian-earliest Asselian), Variscan deformation changes from thin- to thick-skinned (Rodríguez-Fernández and Heredia, 1987; López-Gómez et al., 2019a) giving rise to NW-SE strike-slip faults, such as the Ventaniella Fault (Fig. 2), which was one of the main structures of the Late Variscan deformation (Arthaud and Matte, 1975). The post-Variscan Permian basins of the Cantabrian Mountains have the same trend to the Variscan and Late Variscan structures, they are elongated, narrow and isolated, although some of these appear close to each other and may be interconnected (López-Gómez et al., 2019a). In the Pyrenees, sedimentary and volcanic Permian rocks encompass middle Permian ages and are mainly located around the Paleozoic outcrops of the Basque Massifs (east of VCR) and the Pyrenean Axial Zone (Figs. 1b, 2, 3). In the southern sectors of the Axial Zone, pre-Permian Paleozoic rocks show deformation developed under very low grade to non-metamorphic conditions, so these sectors can be considered part of the Variscan foreland (García-Sansegundo et al., 2011). The Permian basins are elongated and narrow, have a NNE-SSW trend similar to Variscan structures (Fig. 1b), and are separated by areas up to 32–38 km long, constituted by other Paleozoic rocks (Valero-Garcés and Gisbert, 2004). In some cases, the lower-middle Permian sedimentary record of the Pyrenees rests paraconformably on the so-called Gray Unit, a continental succession of Kasimovian-early Asselian age, which rests unconformably over older Paleozoic rocks that were deformed during the Variscan orogeny (Lloret et al., 2018). The Gray Unit is similar to post-tectonic continental Variscan sediments, upper Kasimovian-lower Gzhelian in age (Colmenero et al., 2002), that crop out in the westernmost sectors of the Variscan Cantabrian Zone and in the West Asturian-Leonese Zone (Fig. 1b).

After the Permian, the pre-orogenic stage of the Alpine Cycle continued with a generalized extension during the Early (Pyrenees) to Middle Triassic times (Cantabrian Mountains). Sedimentation was dominated by siliciclastic continental units and related to the opening of the Bay of Biscay, the local result of the Pangea breakup (López-Gómez et al., 2019a, 2021). During the Late Jurassic-Early Cretaceous, a new rifting phase pulse took place, characterized by a thick accumulation (over 10,000 m) of continental and marine deposits (García-Mondejar, 1989). Between the two rifting stages, a thermal subsidence period, dominated by marine carbonates, developed in the northern margin of Iberia (Boillot et al., 1979; García-Espina, 1997; Teixell, 1998; Muñoz, 2002; Capote et al., 2002; Fernández-Viejo et al., 2011; Carballo et al., 2015; Martín-Chivelet et al., 2019; López-Gómez et al., 2019a, 2019b, among others). The second rifting phase is also known as a hyper-extensional event (Tugend et al., 2014; Cámara, 2017) which reactivated the previous structures and individualized the Iberian and the European plates (e.g. Ziegler, 1993). Subsequently, a thermal subsidence phase, mainly developed in Upper Cretaceous times and with predominant marine carbonate sedimentation, preceded a compressional event generated during the Alpine orogeny, which ended with the pre-orogenic stage of the Alpine cycle.

The Alpine orogeny formed the Pyrenean-Cantabrian orogenic belt as the result of oblique convergence and collision of the Iberian and Eurasian plates from the Late Cretaceous in the Pyrenees until the late Neogene (Dewey et al., 1989; Srivastava et al., 1990; Jabaloy et al., 2002; Anderweg, 2002; Martín-González and Heredia, 2011a, 2011b). In the central Cantabrian Mountains, Alpine compression began in the late Eocene and already in the early Oligocene in the western end of these mountains, where the deformation continued until the late Miocene. These ages indicate a westward migration of the deformation, due to the oblique collision (Martín-González et al., 2014; Martín-González and Heredia, 2011b and references therein). Some of the Variscan and late-Variscan faults and many of the Permian and Mesozoic normal faults of the Pyrenean-Cantabrian Mountains were reactivated during Alpine compression (Martín-González et al., 2021 and references therein). In many cases, fault reactivation masked the original extensional structure of the Permian-Mesozoic basin (Vergés and Burbank, 1996; Sinclair et al., 2005; Jolivet et al., 2007; Vacherat et al., 2014; Fillon et al., 2016).

In the southern part of the Pyrenean Axial Zone, Alpine thrusts reactivated some Permian faults and, on other occasions, the Permian faults were folded or tilted by the verticalization of the southern limb of the Axial Zone antiform (Muñoz, 2002, 2019). This is the case of the Somport-Anayet Basin, located in the western Pyrenean Axial Zone (Fig. 3a-d). In the western Cantabrian Mountains, Alpine compression

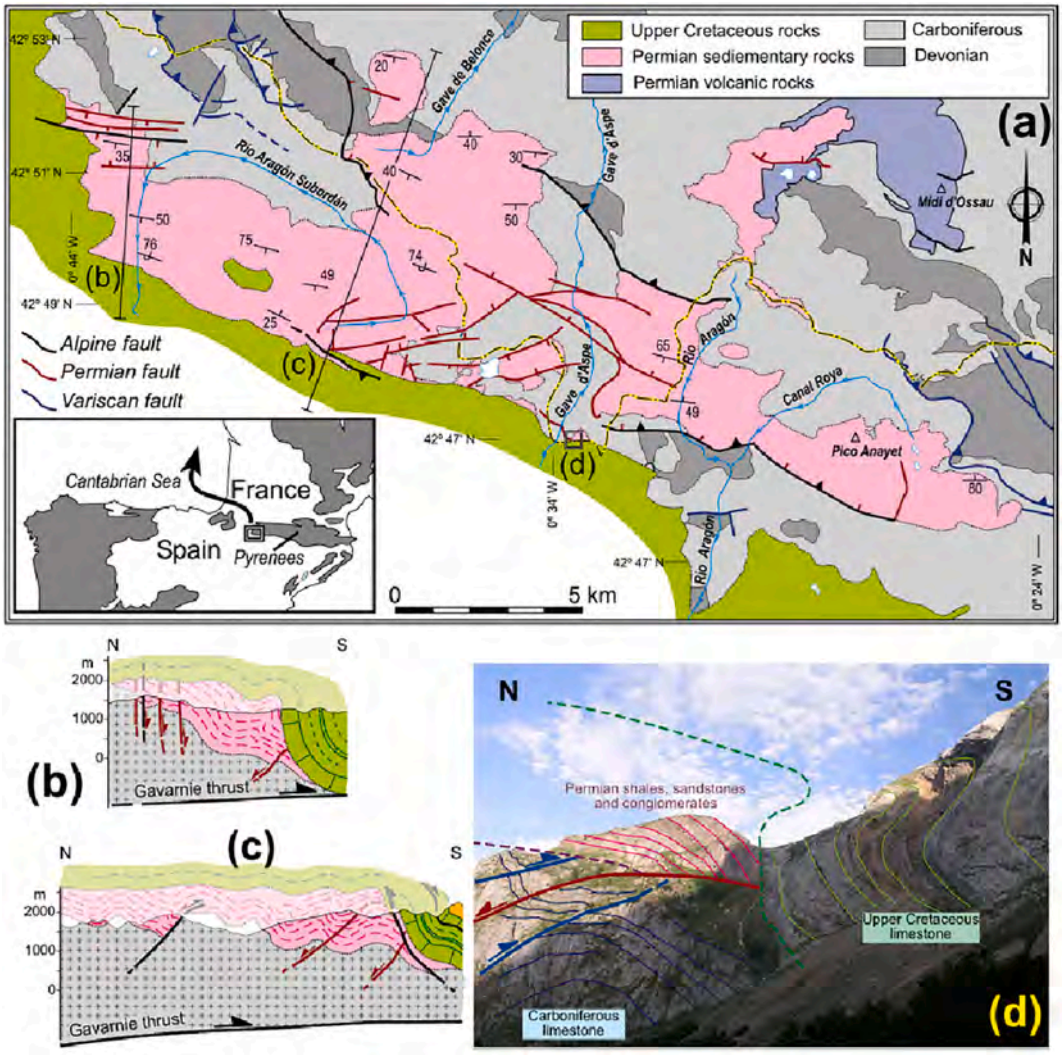

Fig. 3. a) Geological map of the Somport-Anayet basin of the eastern Axial Zone of the Pyrenees showing the Permian outcrops of the TU, LRU and URU lithostratigraphic units (9 in Fig. 2), compiled and based on 1:50,000 scale geological maps of Spain and France (Ternet et al., 2004; Teixell and García-Sansegundo, 1994; Teixell et al., 1994; Ríos et al., 1987). b) Geological cross-section through the western part of the Somport-Anayet basin, where the N-100 E faults that limit the basin to the north are observed. c) Geological cross-section through the central part of the Somport-Anayet where the basin is wider and the limit at its southern edge is marked by N-75E trending faults. d) Photograph showing the Permian sequence on the Gavarnie Alpine thrust frontal ramp; note the tilting of layers and the Permian fault.

was less intense than in the Pyrenees (Alonso et al., 1996; Pulgar et al., 1999). Hence, Permian faults are often only partially inverted, preserving their original geometry (García-Espina, 1997; López-Gómez et al., 2019a, 2021).

3. Methods

This work is based on the study of 12 detailed stratigraphic sections obtained from representative zones of the Pyrenean-Cantabrian orogenic belt. We also examined a borehole core in the westernmost study area (La Camocha Mine), where outcrops are poor and scarce or difficult to access. Detailed field work including sampling, mapping, cross sections, stratigraphy, facies and facies association differentiation was conducted to establish the roles of the main faults and main tectono-sedimentary pulses in the different zones of the study area. Geometries and kinematics of Permian structures were defined by addressing the displacement of Variscan and Permian markers such as bedding folds and fault traces.

Facies and facies associations were differentiated to obtain the main architectural elements and define the depositional systems and their development patterns. Codes of facies follow those defined in Miall's (1996, 2014). Mineralogical and paleosol data were those described recently by our team (López-Gómez et al., 2019a; Lloret et al., 2021) and used to better characterize depositional systems and climate evolution. To establish affinities of the associated volcanism and their relationships with the tectono-sedimentary pulses, mineral assemblages and rock textures were examined in the studied sections, mostly from our recent work (Heredia et al., 2019; López-Gómez et al., 2019a, 2021; Lloret et al., 2021; Martín-González et al., 2021). To constrain unit ages, we used published radiometric data by other authors (Valverde-Vaquero et al., 1999; Pereira et al., 2014; Rodríguez-Méndez et al., 2014). Ages based on palynological assemblages, ichnological and paleobotanical data were obtained mostly from our recent work (Mujal et al., 2016b; López-Gómez et al., 2019a, 2021; Juncal et al., 2019; Lloret et al., 2021).

4. Infill of post-Variscan basins

The stacking pattern of the Permian sedimentary units in the Pyrenean-Cantabrian orogenic belt has been examined in separate geographic areas (Fig. 4). The stratigraphy of the western area, i.e. the

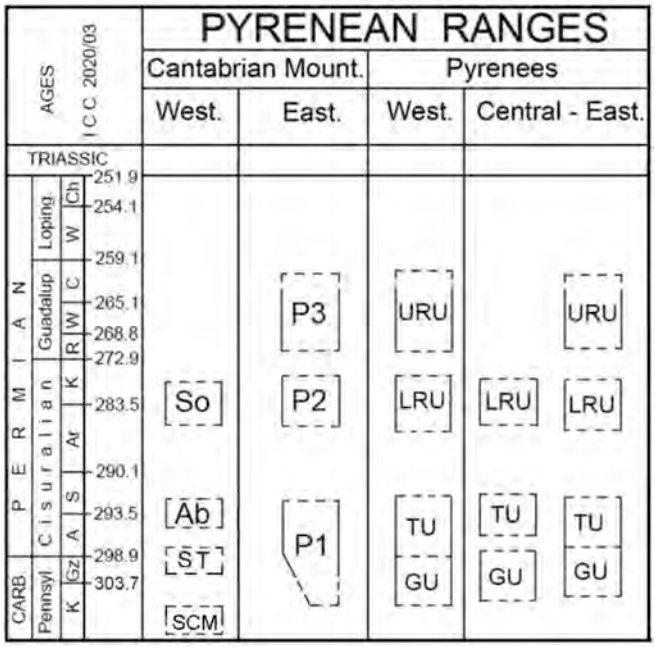

Fig. 4. Permian lithostratigraphic units of the Pyrenean - Cantabrian Ranges: Ab- Acebal Fm; So- Sotres Fm; P1- Permian 1; P2- Permian 2; P3- Permian 3; GU- Gray Unit; TU- Transition Unit; LRU- Lower Red Unit; URU- Upper Red Unit; SCM- Stephanian Cantabrian Mountains; ICC 2020/03- International Chronostratigraphical Chart 2020/03. See text for definitions, descriptions and ages of these units.

Cantabrian Mountains, has been traditionally subdivided into numerous stratigraphic units depending on the study area (Table 1) (e.g., Martínez-García, 1991a; Gand et al., 1997), and traditionally separated from the rest of the Pyrenees by the Pamplona Fault (e.g., Martínez-García, 2004; Valero-Garcés and Gisbert, 2004) (Fig. 1a). Based on new radiometric and paleontological ages and sedimentary evidence, this nomenclature of numerous stratigraphic units was recently re-defined and simplified by López-Gómez et al. (2019a) into two subunits which are not continuous stratigraphically: the Acebal Formation and the Sotres Formation, from older to younger. The Acebal Formation rests unconformably on the San Tirso Formation, of late Carboniferous-early Permian age. Due to the poor quality of outcrops, the Basque area (VCR, Fig. 1a), has been very little described. The Permian sedimentary record in this area was subdivided for the first time in the Maya section, Cinco Villas Massif (Fig. 2 h) by Muller (1969) into three units: P1, P2 and P3, from older to younger. The stratigraphy of the eastern zone, i.e. the Pyrenees s.s., was established by Gisbert (1983) as three units separated by unconformities: Transition Unit (TU), Lower Red Unit (LRU) and Upper Red Unit (URU), from older to younger, resting unconformably on the Gray Unit (GU) of latest Carboniferous age. Gisbert (1983) correlated units P1, P2 and P3 defined by Muller (1969) with GU-TU, LRU and URU, respectively (Fig. 4). This subdivision synthesizes the local nomenclature of this area described by previous authors (e.g., Mirouse, 1959; Mey et al., 1968; Nagtegaal, 1969).

4.1. Stratigraphic units

In the Cantabrian Mountains, the lower Permian succession of the Acebal Formation developed unconformably on the San Tirso Formation (Velando et al., 1975; Wagner and Martínez-García, 1982), which filled a late-Variscan through during the upper Gzhelian-basal Asselian (López-Gómez et al., 2019b). The San Tirso Formation crops out only in a small basin in the La Justa–Aramil Alpine syncline (Fig. 2) and is composed of sandstones, conglomerates and lutites. However, in most of the Cantabrian Mountains, the Permian rests unconformably over the Paleozoic Variscan basement (Martínez-García, 1981).

The Acebal Formation reaches a thickness of 310 m and consists of green volcanic and volcaniclastic rocks, red to green medium-coarse sandstones, and lutites (López-Gómez et al., 2019a). The Sotres Formation, which can attain a thickness of 320 m, has been subdivided into Lower, Middle and Upper subunits (López-Gómez et al., 2019a). This formation rests unconformably on the Acebal Formation or the Variscan basement. It consists of fine-medium sandstones, mudstones and siltstones in the Lower Subunit, limestone in the Middle Subunit affected by a well-developed karst surface at the top, and marls, limestones, mudstones and evaporites in the Upper Subunit (López-Gómez et al., 2021). The mineralogical composition of the Sotres Formation includes illite as the dominant clay mineral, along with quartz and hematite (up to 5%) and may contain up to 20% calcite. In the Middle and Upper subunits of this formation, the clay mineral association also contains chlorite and traces of smectite randomly interstratified with illite (López-Gómez et al., 2021).

The lower stratigraphic unit in the Basque Massif area was defined by Muller (1969) as P1 Unit. It is composed of a 15 m thick alternation of carbonate breccias and limolite beds in its lower part, and fine sandstone and siltstone with reddish colorations and carbonate nodules forming lenticular beds of "calcareous sandstones". The upper part of the P1 consists of reddish siltstones with shale pebble conglomerates. The middle unit, P2, which rests unconformable on unit P1, is about 100 m-thick and represented by a 5–15 m thick bed succession of conglomerates, sandstones and siltstones in its lower part, followed by an alternation of reddish sandstones and siltstones (Muller, 1969; Gisbert, 1983). The upper unit, P3, which rests unconformably on P2 (Mirouse, 1966) may be up to 1200 m thick but with a significant lateral decrease. It is composed of conglomerates of carbonate clasts, sandstones and massive lutites with intercalated volcanic beds (Mirouse, 1966; Gisbert, 1983).

The Permian succession of the Pyrenees rest unconformably on the GU or on the Paleozoic basement (Gisbert, 1983; Valero-Garcés and Gisbert, 2004). The GU includes andesites and ignimbrites and conglomerates and/or breccias at the base, and sandstones, mudstones and siltstones at the top (Gretter et al., 2015; Lloret et al., 2018). This unit, of Kasimovian-Gzhelian (late Carboniferous) age (Pereira et al., 2014; Lloret and Juncal, 2018; Juncal et al., 2019), rests unconformably on the Variscan basement with an angular unconformity. The TU, which represents the first Permian unit in this area, consists of alternating dacites, ignimbrites and tuffs, interbedded with fining-upwards sequences of conglomerates, sandstones and siltstones that may contain interbedded coal beds (Lloret et al., 2018) of Asselian age. The LRU is represented by conglomerates, sandstones and siltstones with well-developed paleosols and locally intercalated limestones and volcaniclastic beds. The URU shows a similar lithology to the LRU, although siltstones and mudstones are more abundant, and conglomerate and limestone beds are less frequent. Both units are separated by an unconformity (Gisbert, 1983) that may appear more attenuated to the east (Gretter et al., 2015). Mudstones and siltstones of the LRU and URU also contain illite as the main clay mineral in addition to chlorite, which is less abundant and reaches slightly higher concentrations in the upper part of the LRU. Quartz, calcite, feldspar and hematite complete the mineralogical association of the clastic sediments (Mujal et al., 2016b; Lloret et al., 2018). The sedimentary evolution of these units is comparable to that of other more local sections within the study area, since there is a clear correlation between all of them, as shown in Table 1.

4.2. Age constraints from radiometric dating and paleontology

The ages for the latest Carboniferous–lower Permian units of the Cantabrian Mountains-Pyrenees are provided in Fig. 4. In the Cantabrian Mountains, the late Carboniferous succession is resting unconformably on the West Asturian-Leonese Zone and western Cantabrian Zone. The

Table 1
Lithostratigraphic units defined in the study area and correlations between them. The units in red have palaeontological or radiometric ages available, and are the ones used in this work (see also Fig. 4). Abbreviations of the units: Cv: Caravias; Ca: Cabranes; So: Sotres; St: San Tirso; Sa: Peña Sagra; Cu: Cuesta; Pa: Paraes; Ar: Arroyo; Ab: Acebal; P1: Permian 1; P2: Permian 2; P3: Permian 3; Gu: Gray Unit; LRS: TU: Transition Unit: LRU: Lower Red Unit; URU: Upper Red Unit; Pera: Peranera; Malp: Malpàs; Erill-: Erill-Castell; Agui: Aguiró; SCM: Stephanian Cantabrian Mountains. References: 1: Martínez-García et al., 1998; 2: Martínez-García, 1981; 3: Martínez-García, 1991a; 4: Martínez-García, 1991b; 5: Manjón et al., 1992; 6: Gand et al., 1997; 7: Robles et al., 2004; 8: Martínez-García, 2004; 9: López-Gómez et al., 2019a; 10: Muller, 1969; 11: Valero-Garcés and Gisbert, 2004; 12: Mey et al., 1968; 13: Nagtegaal, 1969; 14: Gisbert, 1981; 15: Lloret, 2019; 16: Gretter et al., 2015.

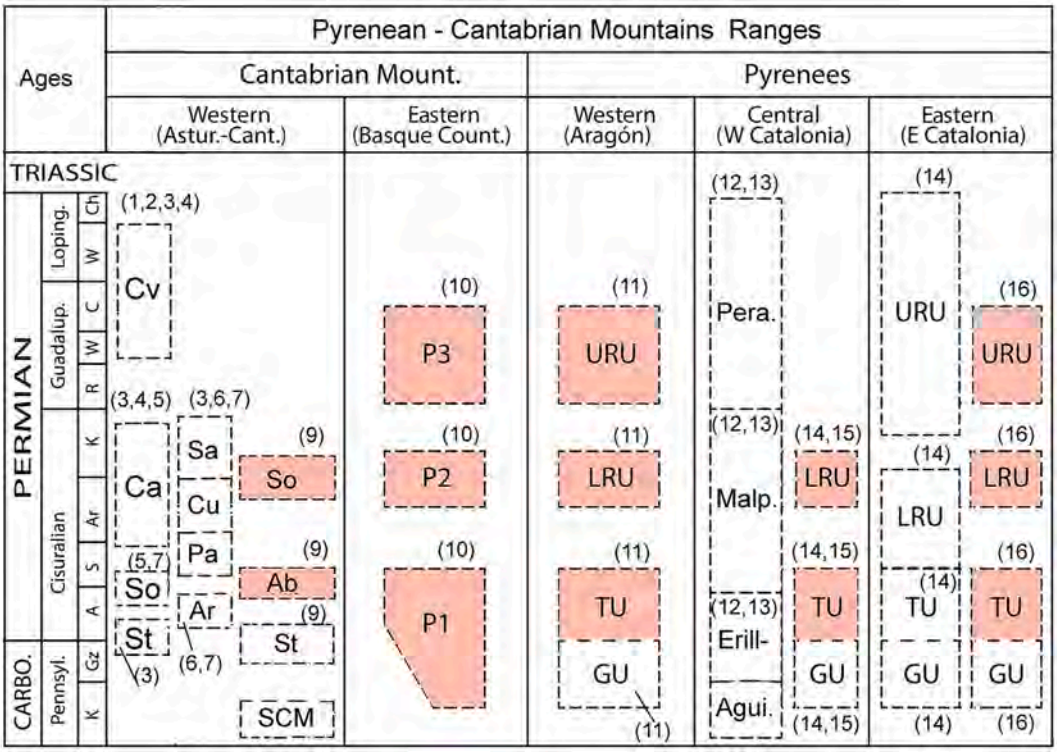

age of this succession is late Kasimovian-early Gzhelian (304.2 ± 1.1 Ma and 302.13 ± 0.23 Ma) based on radiometric data of volcanic ash-fall intercalations (Merino-Tomé et al., 2017). The San Tirso Formation is latest Carboniferous–earliest Permian in age (late Gzhelian-earliest Asselian) (Wagner and Martínez-García, 1982; López-Gómez et al., 2019a and references therein) based on a paleoflora association. In the Pyrenees, the GU was recently dated by Pereira et al. (2014) as Kasimovian-early Gzhelian (304 ± 2 Ma and 300 ± 1 Ma) based on U—Pb dating of zircons from andesites and ignimbrites, and by Juncal et al. (2019) as Gzhelian based on palynological associations. However, according to the ages of similar microflora associations from neighboring European basins, these last authors do not discard a Gzhelian-earliest Asselian age for the GU.

Based on these ages, the GU of the Pyrenees can be correlated with the late Carboniferous succession of the West Asturian-Leonese Zone and western Cantabrian Zone, while the San Tirso Formation of the Cantabrian Mountains, which rests unconformably on this Carboniferous succession, does not have a clear equivalent in the Pyrenees, although it could be assigned to the upper part of the GU.

Until recently, the lack of precise ages for the Permian units of the Pyrenean Ranges has been a considerable challenge to establish detailed correlation among them. New age data for the Cantabrian Mountains have allowed us to update the stratigraphy of the sedimentary succession in this area (López-Gómez et al., 2019a). In the Pyrenees, radiometric ages (Pereira et al., 2014), pollen assemblages (Lloret, 2019) and ichnoassemblages (Mujal et al., 2016a, 2016b, 2018) have also allowed for more precise age constraints. Although there are still ages to be determined in the Permian sedimentary record of the Basque area, some authors have proposed correlations with better known neighboring areas (e.g., Gisbert, 1983; López-Gómez et al., 2002, 2019b).

The age of the Acebal Formation (ca. 297–292 Ma, Asselian-early Sakmarian) in the Cantabrian Mountains has been inferred from those of related magmatic rocks determined by U—Pb analysis near the villages of Infiesto-Siero (Valverde-Vaquero et al., 1999), 3.5 km eastwards of the Acebal section (Fig. 2). Based on palynological data, the Sotres Formation is late Artinskian–early Kungurian (Juncal et al., 2016; López-Gómez et al., 2019a).

For the TU in the Pyrenees, ignimbrite rocks in the Erill Castell section have been dated as Asselian (U—Pb zircon age 297 ± 3 Ma; Pereira et al., 2014). According to the macroflora (Dalloni, 1930), the lowermost part of this unit could be extended to the latemost Stephanian C (Gretter et al., 2015). The age of the LRU is Artinskian (290 ± 1 Ma and 286 ± 2 Ma) according to U—Pb radiometric data obtained in the Castellar de N'Hug section (Pereira et al., 2014). Macroflora and plant remains from the so-called "Flora of Gotarta" (Broutin and Gisbert, 1985), together with ichnoassemblages (Mujal et al., 2016a) and a palynological analysis (Juncal personal com., in Lloret, 2019) also support this age. The age of the URU is based on less precise criteria and therefore spans a wider range. Data from tetrapod footprints (Robles and Llompart, 1987; Mujal et al., 2016b, 2018) indicate a Guadalupian (possible Wordian) age. However, as discussed later, the results of recent magmatism (U—Pb zircon datings) studies could extend this age to the Capitanian.

The Basque area of the Pyrenean Ranges has no direct age

determinations in its lower Permian sedimentary succession. As discussed below, the correspondence between P3 and URU may be supported by indirect radiometric data.

Based on these ages, the P1/TU and P2/LRU units of the Pyrenees can be correlated respectively with the Acebal and Sotres formations of the Cantabrian Mountains, while the P3/URU units have no equivalent in the Cantabrian Mountains (Fig. 4).

5. Sedimentary evolution

Twelve representative lithostratigraphic sections across the study area were described to examine the sedimentary evolution of the different sectors (Fig. 2). Field observations were complemented with data from one borehole in the westernmost area because of difficult access to the lower Permian rocks or access is difficult (Fig. 5).

5.1. Depositional environments

After defining 24 (1 to 24) facies in the field, these were grouped into 15 facies associations (Fig. 6). Depositional environments in the different stratigraphic units were defined based on vertical stackings of these facies associations in the studied sections (Fig. 5). These associations show three main depositional environments (Fig. 6): A- fluvial, B- lacustrine and palustrine and C- volcaniclastic.

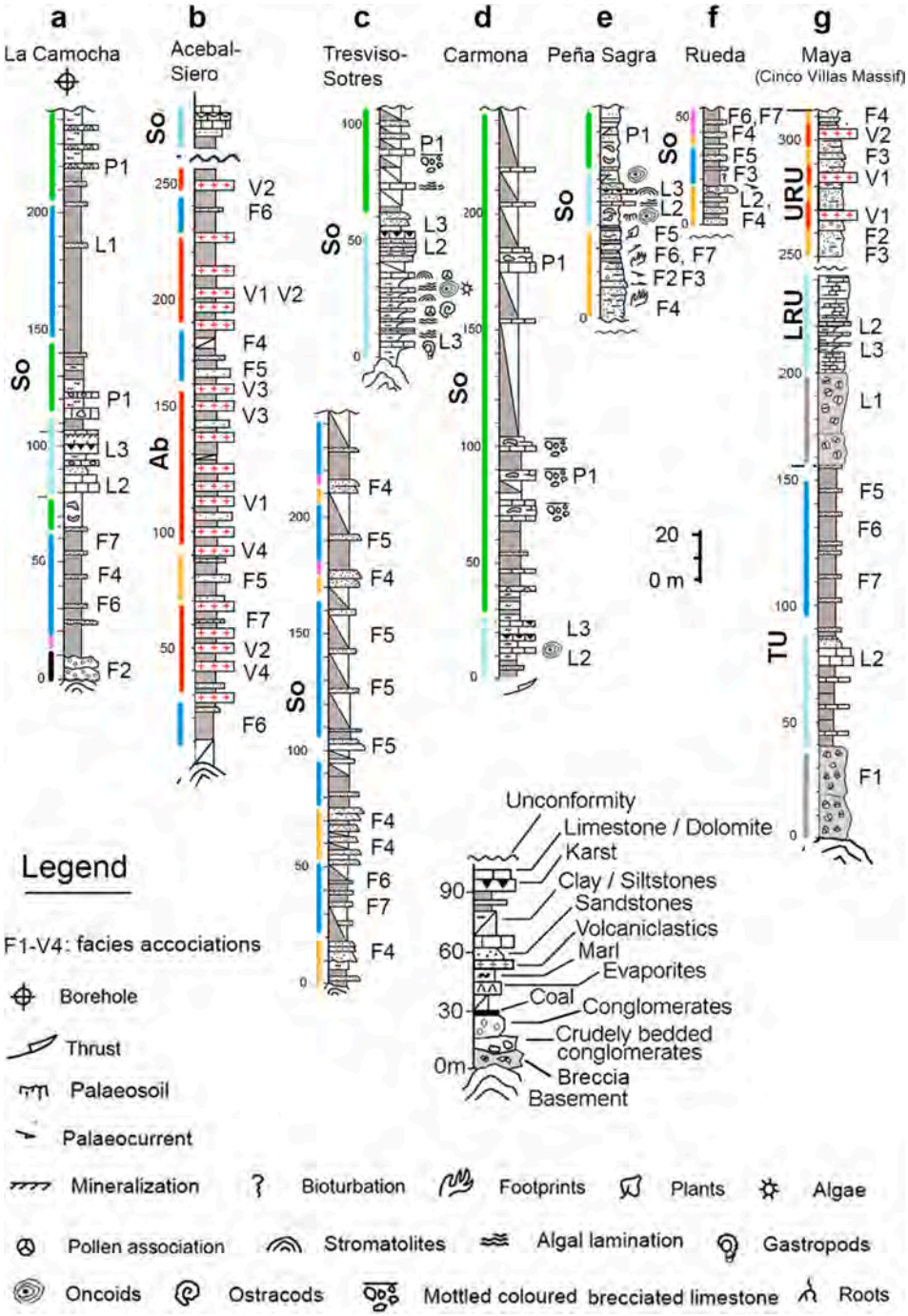

Fig. 5. Twelve examined sections (b - m) and the La Camocha borehole (a). See locations in Fig. 2. Sections show lithological units with their facies associations and main depositional systems. See data of facies and facies associations in Fig. 6 and their description and interpretation in the text.

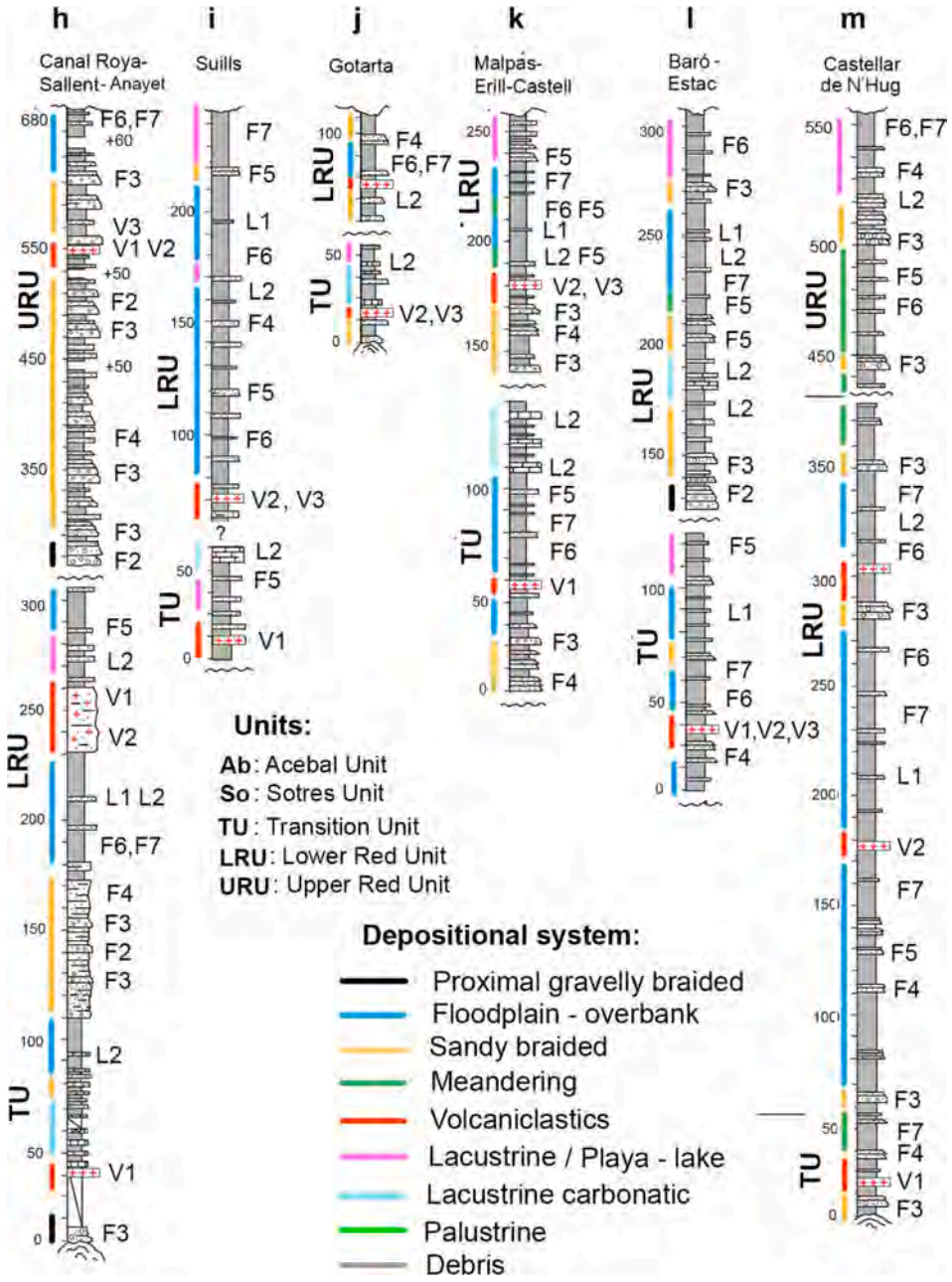

Fig. 5. (*continued*).

A- *Fluvial depositional environment*: represented by facies associations F1 to F7 (Fig. 6). Three main subenvironments were identified: high-strength and viscous (local) deposits (F1), channel fill (F2 – F5), and overbank (F6 – F7). Facies association F1 (Fig. 7 a) is composed of coarse-grained massive poorly-sorted deposits. The sheet-like characteristic of this association indicates deposits from unconfined or confined high-density currents (De Haas et al., 2016). Facies associations F2 to F5 feature fining-upward sequences less than 5 m thick. They show gravel and sandstone bars, and bedforms with 2D—3D cross-stratification (F2 and F3 facies associations, Fig. 7 b and c, respectively) reflecting braided fluvial systems in single- or multi-storey sheet sandstones, similar to those described by Colombi et al. (2017) for the Upper Triassic Ischigualasto Formation of NW Argentina. Deposits related to abandoned channels are shown in the upper part of some sequences of facies associations F4, where incipient soils may develop on massive mud deposits, similar to those described by Gulliford et al. (2017) for the Permian-Triassic Beaufort Group, South Africa. Sheets characterized by lateral accretion surfaces constitute the main body of facies association F5 (Fig. 7 d). The upper part of this association is represented by abandoned channel deposits, whereby thin fine-sand beds with ripples and desiccation-cracks may develop at the top of the sequence. This facies association represents channel-fill in meandering fluvial systems, similar to examples described in the late Cretaceous Mancos Formation, south-central Utah, USA (Wu et al., 2016) and the lower Permian Clear Fork Formation, north-central Texas, USA (Simon and Gibling, 2017). Overbank deposits are represented by facies associations F6 and F7 and constitute the dominant subenvironment of the fluvial depositional system. They mostly show massive or fine-laminated siltstones interbedded with thin beds of medium to fine-grain sandstones (Fig. 7 e) featuring small-scale cross-lamination, ripples, bioturbation, plant remains, paleosols and desiccation cracks (Fig. 7 e, f). These are interpreted as distal crevasse-splay deposits on floodplains. Facies association F7 can also show coal beds up to a few meters thick deposited in swamps. These facies associations commonly show vertical

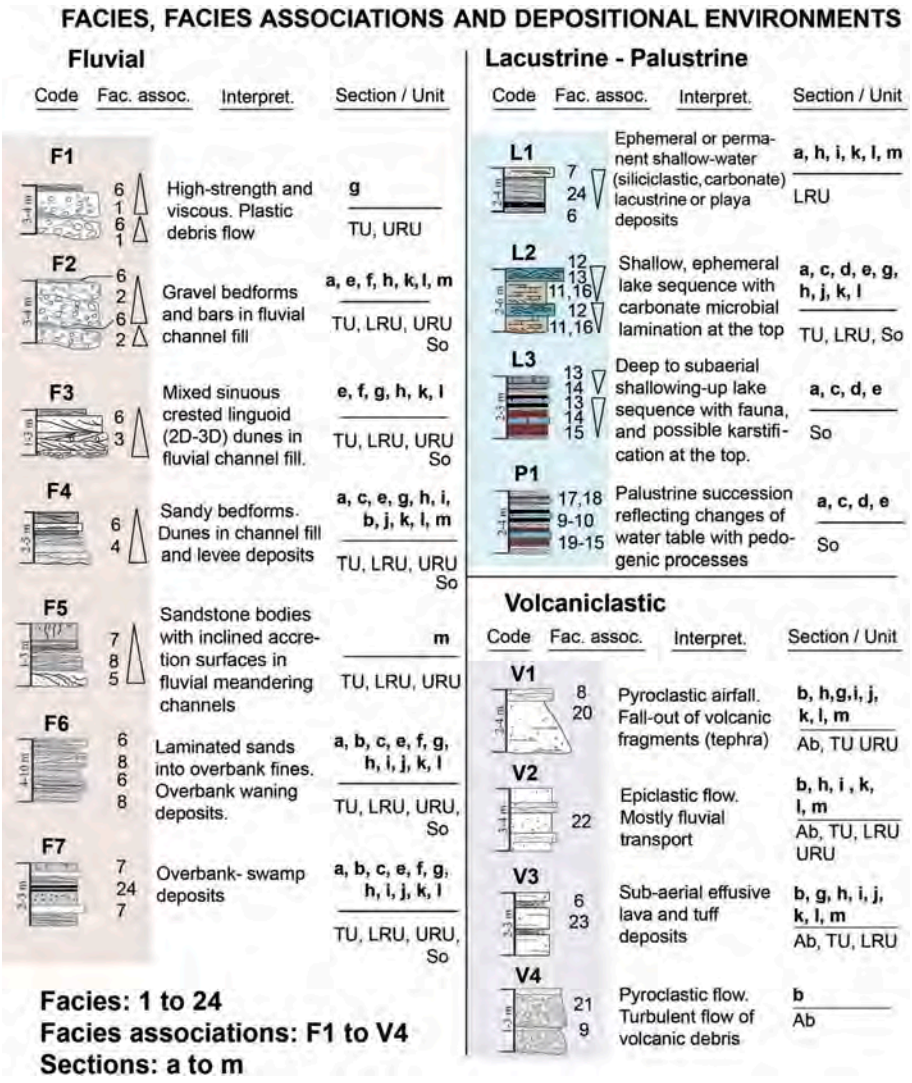

Fig. 6. Facies (1 to 24) and facies associations (F1 to V4). Facies.- 1: Oligomictic clast-supported conglomerates or breccias, weakly grading and poorly rounded clasts up to 20 cm; 2: Clast-supported bedded gravel. Trough and planar cross-beds; 3: Sand, fine to very coarse, and pebbly with trough and planar cross-beds; 4: Fine to medium sand with planar cross-beds; 5: Fine to coarse sand with cross-beds (possible epsilon crossbedding); 6: Fine to medium sand (dm-thick beds) with small-scale cross-stratification, parallel lamination and ripples alternating with massive mud-silt deposits with roots (paleosols); 7: Massive mud-silt with desiccation cracks, plant remains and roots (paleosols), and/or bioturbation; 8: Alternating medium to fine sands and silts with fine lamination and ripples; 9: Massive muds and thin beds of fine sand, dolomite or evaporites deformed by soils, and carbonate nodules; 10: White limestones or fine-grain calcarenite with small-scale planar cross-lamination; 11: Sandy limestone beds with oncoids and small ripples; 12: Carbonate microbial lamination that may occur as domes; 13: White massive carbonate beds with possible karstic surfaces; 14: Poorly rhythmic laminated muddy beds with ostracods, gastropods and algae; 15: Laminated dark limestones constituting cm-thick beds; 16: cm-thick well-stratified limestone with small-scale cross-beds and shell fragments; 17: Mottled silts intercalated with laminated limestones that may show domal structure; 18: Alternating fine wavy beds of mottled marls, muds, limestones and evaporites with possible bioturbation by roots, and coated (pedogenic) grains; 19: cm-thick wavy levels of alternating green marls with high organic matter contents and limestones disrupted by roots; 20: Graded pyroclastic lapilli-breccia deposits; 21: Reworking of volcaniclastic material with soft structures; 22: Medium-thick structureless volcanic massive beds of volcanic rocks; 23: Volcanic lava with intercalated muds of fine sands; 24: Rhythmic lamination of silt and fine sand with plant remains and intercalations of thin beds of coal.

alternation with sandy single- and multi-storey sheets, represented by facies associations F3 and F4, in a similar succession to examples described by Burns et al. (2017) in the Cretaceous Nelsen Formation.

B- *Lacustrine and palustrine depositional environments*: represented by facies associations L1 to L3 and P1 (Fig. 6). Facies association L1 is composed almost entirely of massive siltstones with flat laminations and fine-grained massive-crude laminated sandstone at the top. This succession constitutes a coarsening upwards sequence that may be up to 10 m thick (Fig. 7 h). Massive and laminated siltstones indicate settling of suspending sediment in a lacustrine environment, while the modest thickness of the association points to a marginal setting in a shallow-lake environment (Liesa et al., 2000). Facies associations L2 and L3 are related to carbonate lacustrine sequences (Fig. 7 i and l, respectively). Both show shallowing and coarsening–upwards sequences, up to 2.5 m thick, with the carbonate term at the top that may contain karstification surfaces mainly in facies association L3 (Fig. 7 k). The carbonate deposits may show oncoids and microbial lamination that could appear as dome structures developed in shallow semi-permanent or ephemeral lakes (L2), similar to examples described for recent rift basins in Africa (e.g., Frostick and Reid, 1986; Williams et al., 1986) or Permian continental basins in the Southern Alps, Italy (Berra et al., 2019). Occasionally, these lakes may develop in deeper environments and contain dark laminated micrite limestones, ostracods and gastropods (L3). Ostracods and gastropod micrite beds are common in relatively deep low-energy lakes (Murphy and Wilkinson, 1980; Platt and Wright, 1991) and these may be assigned to the "permanent lake microfacies" described by Abels et al. (2004). Facies association P1 consists of mm-cm thick alternating beds of massive or slightly undulated white limestone, red mudstone and marl which are locally disrupted by roots (see also Valero-Garcés and Gisbert, 1992). In the upper part, this association shows an alternation of mm-thick beds of clayey limestone containing small current and wave ripples, root mats, intercalated marl, and evaporite lenses (Fig. 7 j). Clayey limestone may show coated (pedogenic) grains, oncoids and carbonate microbial lamination. This succession may be 4 m thick; it records a palustrine deposition with changes in the water table and modifications to the primary facies through pedogenic or diagenetic processes (e.g., Alonso-Zarza and Wright, 2010; Alonso-Zarza et al., 2012).

C- *Volcaniclastic depositional environments*: represented by facies associations V1 to V4 (Fig. 6). Facies association V1 consists of graded pyroclastic lapilli-breccia deposits that may show horizontal lamination and low angle cross-beds (Fig. 7 m).

Tuff reworking may occur between eruptive periods, appearing within small fluvial channel-fills (Smith, 1987). As a result of the fluvial transport of these deposits, stacking of cm-thick beds of micro-breccias or structureless massive beds may appear, representing epiclastic flows (V2). Pyroclastic flows may also produce turbulent flows of volcanic debris giving rise to unsorted massive matrix-supported breccias (V4) (Fig. 7 n), likely the result of primary, *syn*-eruptive volcanic deposition (e.g., Arguden and Rodolfo, 1990; Breitkreuz et al., 2001).

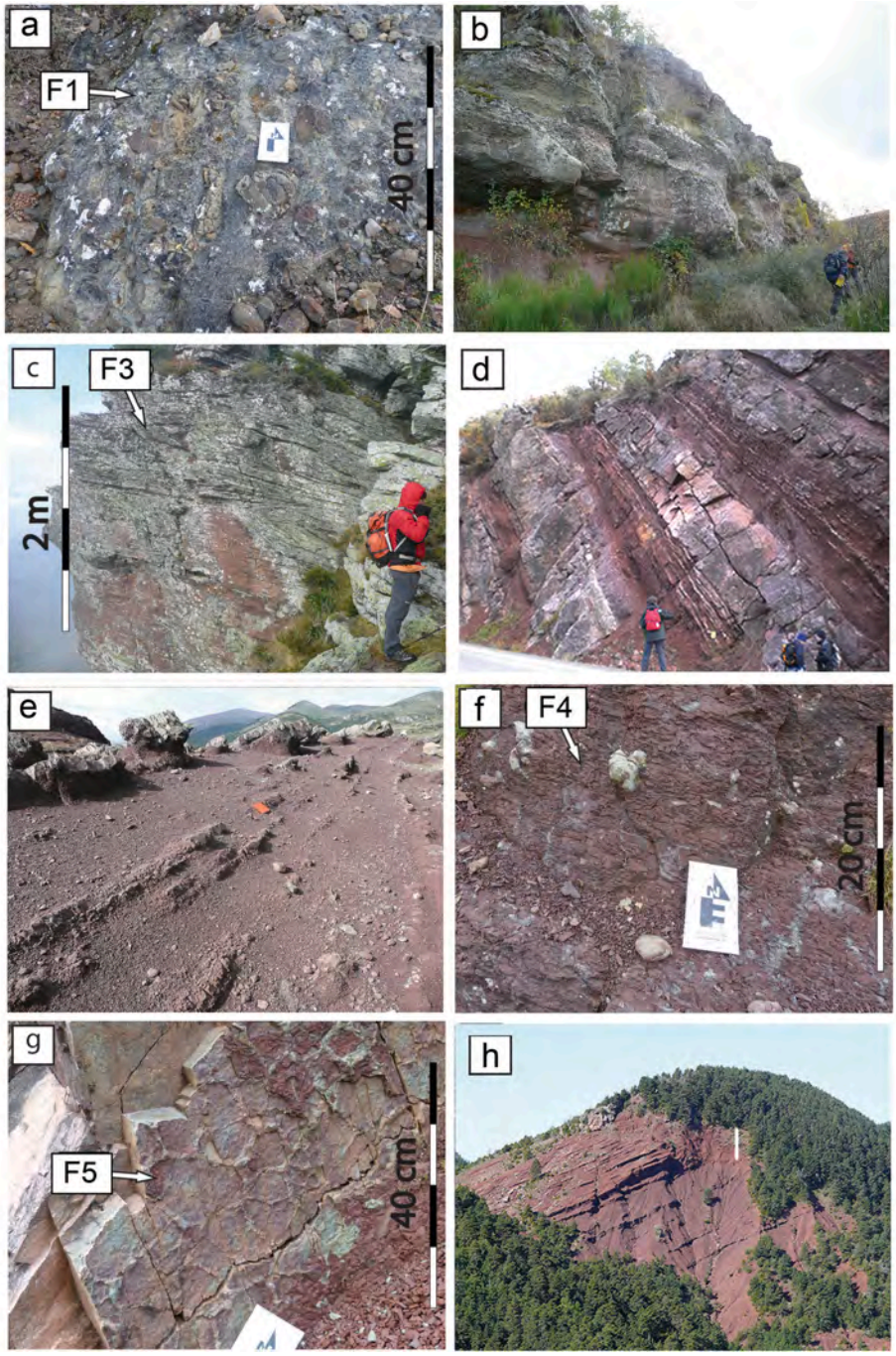

Fig. 7. Field photographs of the facies associations. See Fig. 6 for their description and interpretation. Scales: e- notebook (in the centre of the image): 20 cm; i- hammer: 32 cm; k- backpack: 42 cm.

Sub-aerial effusive lava and tuff deposits may be interbedded with massive mud-silt deposits with paleosols and fine to medium cm-thick sand beds (V3). Although macroscopic features of lava and tuff deposits normally include massive beds, occasionally cm-thick normal graded tuff layers appear, as in the examples described by Stolhofen and Stanistreet (1994) for the Permo-Carboniferous Saar-Nahe, SW Germany.

5.2. Paleopedology

Few studies have examined paleosols of lower and middle Permian deposits in the Cantabrian Mountains and Pyrenees (e.g., Gascón-Cuello and Gisbert, 1987; Lloret, 2019; López-Gómez et al., 2019a, 2021; Lloret et al., 2021). Along with sedimentary data and the isotopic record of $\delta^{18}O$ and $\delta^{13}C$, based on these studies of paleosols, we can infer the climate evolution trend in the units analyzed here.

In the Cantabrian Mountains, four pedotypes showing a clear vertical distribution have been identified in the Sotres Formation (López-Gómez et al., 2019a, 2021). Three of them were observed in alluvial facies associations F6 and F7 of the lower part of this unit, and one at the top of the alluvial-lacustrine-palustrine facies association P1. Isotopic records of $\delta^{18}O$ and $\delta^{13}C$ on calcareous pedotypes, typical of the lower portion of the unit (López-Gómez et al., 2021), indicate arid and semi-arid conditions with high seasonality, related to monsoon climate conditions. The

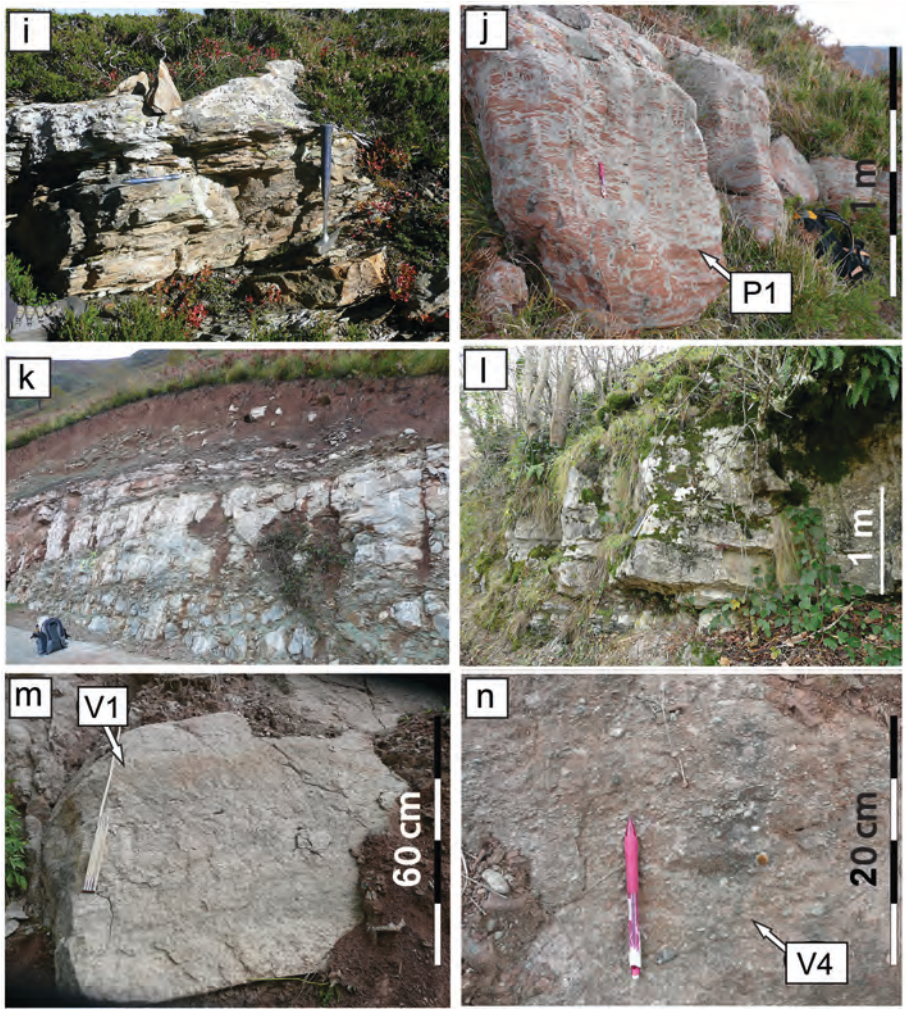

Fig. 7. (*continued*).

presence of calcretes in facies association P1 of the upper part of the Sotres Formation (Fig. 8A) suggests greater climatic stability. The sedimentary environments of these latter soils in the Sotres Fm in the Cantabrian Mountains represent the transition from exposed surfaces to shallow water bodies (López-Gómez et al., 2021).

In the Pyrenees, Lloret et al. (2021) detailed the course of pedogenic evolution in alluvial facies associations F6 and F7 of the LRU and URU units. Paleosols related to arid- and sub-arid conditions (Aridisol, Entisol and Inceptisol) were described in the fluvial and lacustrine environments of the LRU (Fig. 8B). These environments developed under a pronounced topography and monsoon climate. The paleosols of the URU show reduced maturity and a greater presence of water than those of the

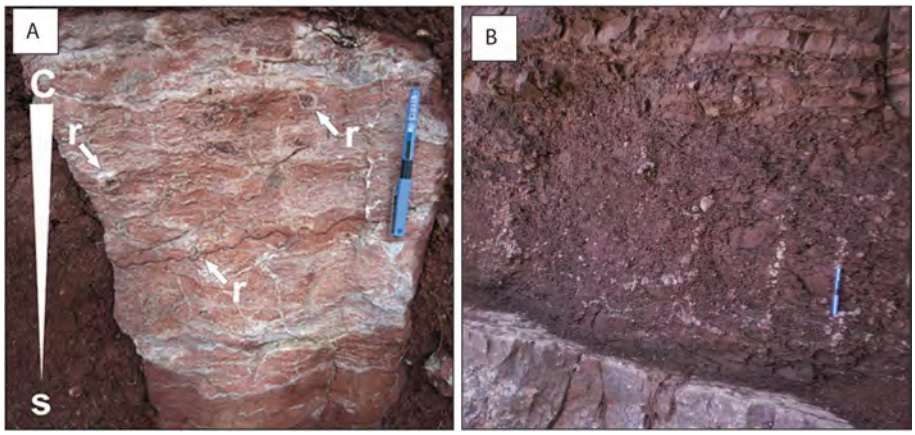

Fig. 8. Examples of paleosols in the studied units. A) Palustrine carbonate at the initial stage of carbonate accumulation in the upper part of the Sotres Formation (Carmona section), Cantabrian sector. Note the higher carbonate content (C) at the top of the profile replacing the silty/sandy material (s) and the intercalated roots (r). B) Carbonated roots in a silty bed of overflood deposits in the LRU, eastern Pyrenees (Baró-Estac section).

LRU. The inferred climate of these paleosols indicates less arid conditions than those inferred for the LRU.

5.3. Sedimentary evolution of the units

The vertical and lateral evolution of depositional systems in the studied units is shown in Fig. 9. This figure was prepared by separating the complete sedimentary record of the studied units from periods without sedimentation and/or erosion, as shown in Figs. 4 and 5. Having differentiated the units in time and space, the depositional systems can be seen in their lateral distribution in Fig. 9.

We identify three sedimentary stages, although the youngest is not shown in the Cantabrian Mountains and only appears in some areas of the Pyrenees. The first phase, characterized by alluvial and volcaniclastic deposits, is represented by the Ab, P1 and TU units, of Asselian-Sakmarian age. These units were deposited in small basins related to the still existing lower Permian paleorelief in both the Cantabrian Mountains and Pyrenean areas. The alluvial sedimentary record was mostly related to superimposed and/or isolated channelized conglomerate and sandstone sheets. These were associated with proximal-distal low-sinuosity fluvial systems interbedded with overbank deposits where some paleosols developed. In the Pyrenees area, lacustrine deposits, mostly dominated by carbonate and sometimes related to coal beds, appear in the middle and upper parts of the units. Thick breccia deposits related to proximal deposits also accumulated in the westernmost part of this area.

A second stage of sedimentation, of late Artinskian-early Kungurian age, and still conditioned by local paleoreliefs, mainly comprises alluvial and lacustrine deposits, and is represented by the Sotres, P2 and LRU units (Figs. 4, 9), which were deposited after a period without sedimentation and/or erosion (López-Gómez et al., 2019b). In the Pyrenees, this sedimentary record shows intercalations of volcaniclastic deposits in its middle part, and lacustrine deposits in its upper portion. The lacustrine deposits were mainly carbonate in the Cantabrian Mountains and siliciclastic rocks in the Pyrenees. The top of the carbonate lacustrine deposits in the Sotres Formation of the Cantabrian Mountains is represented by a karstic complex extending laterally over more than 100 km, indicating a long-exposed surface (López-Gómez et al., 2021). The alluvial deposits are related to superimposed isolated channelized sandstone sheets. They are associated with proximal-distal fluvial systems of low and high sinuosity, interbedded with overbank deposits where paleosols developed. In both the Cantabrian Mountains and Pyrenees, the sedimentary record reveals a clear vertical succession from alluvial to lacustrine. In the Pyrenean region, however, intercalated volcaniclastics were very common at this stage, while in the Cantabrian Mountains, palustrine environments widely developed in the uppermost

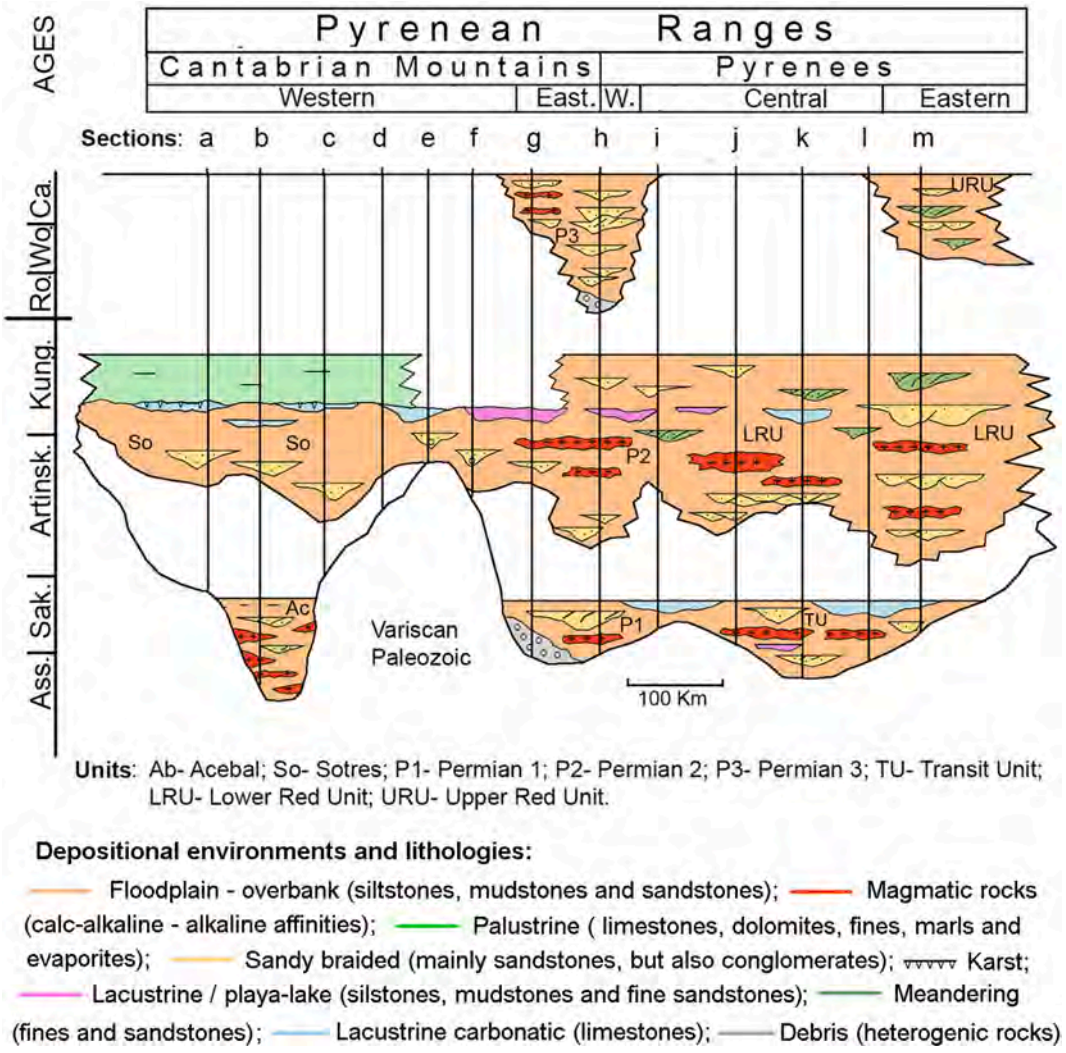

Fig. 9. Temporal and spatial reconstruction of vertical and lateral development of the studied units and their depositional systems in the Pyrenean–Cantabrian orogenic belt. The interval lacking sedimentation and/or erosion is also shown. See Fig. 2 for the geographical location of the sections, and Fig. 5 for details on the sections.

part of the succession.

Due to a lack of sedimentation in the Cantabrian Mountains (López-Gómez et al., 2019a) along with substantial erosion and/or a non-deposition period during the middle-upper Permian and Early Triassic in the Pyrenees (Lloret et al., 2020), the third sedimentary stage, of Roadian-Capitanian (middle Permian) age, is only recorded in few sections of the western and eastern Pyrenees, and is represented by the P3 and URU units (Fig. 9). This sedimentary record mostly reflects high- and low sinuosity fluvial systems with abundant overbank deposits where paleosols developed. Volcaniclastic rocks are also very common, especially in the Maya area of the western Pyrenees (section G in Fig. 5).

6. Magmatism

The Permian magmatism of the Cantabrian Mountains and Pyrenees includes volcanic and plutonic rocks that crop out across the entire mountain chain (Figs. 2, 10). Most plutonic rocks are well preserved, and usually intrude as small stocks (i.e. Peña Prieta area, Fig. 2; Gallastegui et al., 1990), and are more frequent to the west of the orogen. In contrast, volcanic rocks are usually not well-preserved due to weathering, hydrothermal alteration or very low-grade metamorphism. The Permian magmatism in the Pyrenees has been extensively described in the regional literature (see review in López-Gómez et al., 2019b and references therein). Many studies have focused on stratigraphic position and petrology, but absolute ages are scarce. Recent radiometric efforts have provided new constraints on the age of this magmatism (Denèle et al., 2012; Pereira et al., 2014; Fig. 10).

Based on a compilation of age and petrological data (Fig. 10), the Permian magmatic rocks can be grouped into three consecutive magmatic episodes. The first and second episodes share a calc-alkaline geochemical signature, whereas the geochemistry of the third episode is alkaline, suggesting that the change to a extensional regime led to melt generation at higher mantle depths (Bixel, 1988; Broutin et al., 1994; Lago et al., 2004a; Galé, 2005). This geodynamic transition is constrained at the scale of western Paleo-Europe (Cortesogno et al., 1998; Bonin, 1990; Deroin and Bonin, 2003).

Preceding these three episodes, the oldest magmatic rocks are exposed in both the western (AGR in Fig. 1, and section b in Fig. 5) and eastern (El Cadí basin, Fig. 2, Gisbert, 1981) parts of the orogen and are of upper Pennsylvanian (Carboniferous) age (Valverde-Vaquero et al., 1999; Fernández-Suárez et al., 2000; Pereira et al., 2014). They have been classically included as part of the Permian magmatism and related to those of Asselian-Sakmarian age (Fig. 10). Their affinities are shoshonitic to calc-alkaline and are related to melting of the lower crust with variable involvement of mantle melts (Fernández-Suárez et al., 2000; Pereira et al., 2014).

During the first episode (Asselian-Sakmarian), lithospheric melts intruded the Paleozoic basement as stocks in the western part of the chain, namely: the Salas-Belmonte stock (18 km west of the city of Oviedo), and the Peña Prieta stock (Fig. 2). These plutonic intrusions comprise calc-alkaline rocks ranging from gabbros to leucogranites (Gallastegui et al., 1990; Suárez et al., 1993, 1999). In the Axial Zone of the Pyrenees, several intrusions belong to this episode, including the Bossost and Lys-Caillaouas granitoids (López-Sánchez et al., 2019) and the Maladeta and Saint Laurent-La Jonquera granites (Evans et al., 1998; Denèle et al., 2014). Coeval volcanic and volcaniclastic rocks occur interbedded in the Asselian-Sakmarian series in several Permian basins throughout the entire chain (Fig. 10). Excellent examples of these volcanics can be found, from west to east, in the basins La Justa-Aramil, Villaviciosa, Peña Labra, Acebal-Siero, Castejón-Laspaúles, Erill Castell-Malpás and Estac-Baró (Figs. 2, 10). In all these basins, Permian sediments are interspaced by lava flows with compositions ranging from pyroxene- or amphibole-bearing andesites to rhyolites and volcaniclastic rocks deposited from ashfall, pyroclastic surges and ignimbrites (Pereira et al., 2014; Lloret et al., 2018; López-Gómez et al., 2019a). These volcanics also have a calc-alkaline affinity linked to mixed sources including crustal and lithospheric mantle components (Innocent et al., 1994; Lago et al., 2004a; Pereira et al., 2014). The shared calc-alkaline geochemical affinity, together with available ages for this first episode, suggest a petrogenetic link between plutonic and volcanic rocks as proposed by Lago et al. (2004a) and Pereira et al. (2014).

The second and third episodes occur only in the central and eastern parts of the Pyrenees. This younger magmatism has not been described in the Cantabrian Mountains (Fig. 10). The second episode is represented by volcanic rocks and some subvolcanic dykes of calc-alkaline affinity, and took place during the Kungurian (Lago et al., 2004a). In the central part, this episode is exposed in the Somport-Anayet basin as the Midi d'Ossau Permian volcano (Fig. 3a). The base of this volcanic structure and its associated ring dyke is made up of peraluminous dacites and rhyolites (Bixel, 1988; Briqueu and Innocent, 1993; Innocent et al., 1994). The rest of the volcanic structure and summit of the Midi d'Ossau peak consist of andesites that evolved from basaltic andesites to felsic andesites with time (Bixel, 1988; Briqueu and Innocent, 1993). These felsic andesites also occur at the base of the Anayet volcanic massif (Bixel, 1988; Galé, 2005; Lago et al., 2004a). In the eastern part, the second episode is represented by ignimbrites of the Castellar de N'Hug (Pereira et al., 2014) (Figs. 5 m, and 10). With regard to the hypovolcanic rocks of this episode, several dykes of calc-alkaline lamprophyre (spessartites) have been described intruding the Panticosa pluton (Gil-Imaz et al., 2012) and the Maladeta Plutonic Complex (Arranz, 1997), although their age remains unknown. A similar spessartite dyke in the Lys-Caillaouas massif, French Pyrenees, has been dated consistently as Kungurian (Majoor, 1988) (Fig. 10).

The third episode (Wordian-Capitanian?) is only found in the central

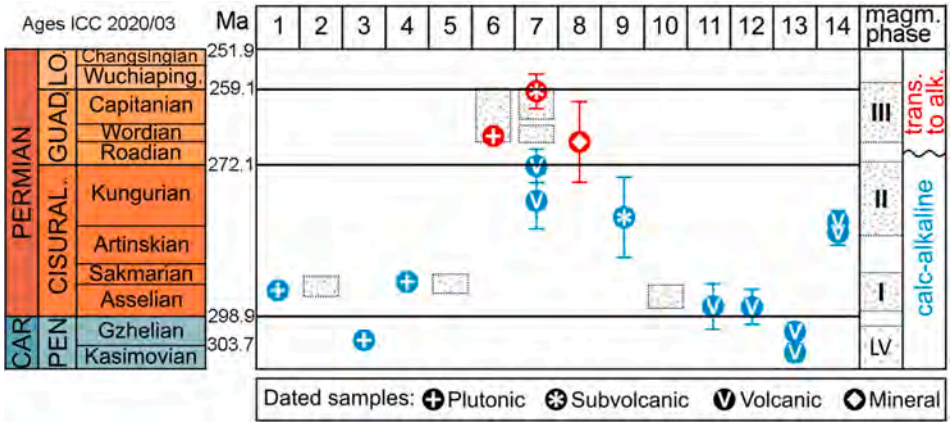

Fig. 10. Compilation of age and geochemical data for the Permian magmatism in the Pyrenean–Cantabrian orogen belt. 1: Salas-Belmonte Stock, 2: Acebal-Siero section, 3: Infiesto Plutonic Complex, 4: Peña Prieta Stock, 5: Peña Labra Basin; 6: Cinco Villas Massif, 7: Somport-Anayet Basin, 8: Panticosa Pluton, 9: Lys-Caillouas Massif, 10: Castejón-Laspaúles Basin, 11: Erill Castell-Malpás Basin, 12: Estac-Baró Basin, 13: Cadí Basin, and 14: Castellar de N'Hug Basin. Radiometric dating: 1, 3, 4 (U—Pb in zircon and titanite by Valverde-Vaquero et al., 1999); 6 (U—Pb in zircon by Denèle et al., 2012); 7 (U—Pb in zircon by Briqueu and Innocent, 1993; Rodríguez-Méndez et al., 2014); 8 (K—Ar in amphibole megacrysts by Debon and Zimmermann, 1993); 9 (K—Ar in biotite and whole-rock by Majoor, 1988); 11–14 (U—Pb in zircon by Pereira et al., 2014). Magmatic outcrops located in Fig. 2.

part of the Pyrenees, in the Cinco Villas-Maya Massif and Somport-Anayet-Canal Roya basin (Figs. 5 g, h and 10). This magmatism has a transitional to alkaline affinity and is again exposed as both plutonic and volcanic lithologies. Plutonic rocks correspond to the Aya pluton in the Cinco Villas Massif (Fig. 10). They range between gabbros and leucogranites and were emplaced during the Wordian (Denèle et al., 2012). Most rocks of this episode are volcanic and show less evolved compositions (trachyandesites, basalts) than the previous episodes. This feature has been related to extensional tectonics, thinning of the crust, and consequent melting of the deeper asthenospheric mantle at lower melting rates than previous magmatisms (Lago et al., 2004a; Galé, 2005). The volcanic rocks of the Cinco Villas Massif are interbedded within Permian sediments, below the unconformity with the basal conglomerates of the Early Triassic units. These volcanics comprise alkali basalts with phenocrysts of olivine and Ti-rich augite (Galé, 2005), and share geochemical features with the gabbros of the Aya (Cinco Villas Massif) pluton. This led Denèle et al. (2012) to suggest that the Aya pluton represents the deep expression of this volcanic episode. The volcanic rocks of the Somport-Anayet basin can be divided into two subunits: alkaline trachyandesites with chromiferous diopside and edenite-pargasitic amphibole (Debon et al., 1996) and alkaline basalts with olivine and Ti-rich augite, similar to those of the Cinco Villas Massif (Galé, 2005; Lago et al., 2004a). These rocks have not been dated yet, however the emplacement of a compositionally similar dyke of diabase intruding the Paleozoic basement in the nearby Sallent area has been dated at 259.2 ± 3 Ma, (U—Pb zircon dating by Rodríguez-Méndez et al., 2014). Finally, amphibole megacrysts carried by alkaline lamprophyres in the Panticosa pluton, 5 km east of Anayet, were dated via K—Ar geochronology by Debon and Zimmermann (1993), providing an age consistent with Wordian-Capitanian crystallization (Fig. 10).

The late Carboniferous magmatism (ca. 310–300 Ma, U—Pb zircon dating by Fernández-Suárez et al., 2000 and Pereira et al., 2014) is related to initial phases of lithospheric delamination (initial orogenic collapse) in the Variscan hinterland (Gutiérrez-Alonso et al., 2011 and references therein). In contrast, the lower Permian calc-alkaline magmatism is related to the final collapse of the Variscan orogen (Ziegler and Stampfli, 2001; McCann et al., 2006; López-Gómez et al., 2019a). The middle Permian alkaline magmatism, restricted to the western Pyrenees, represents the transition to a rifting stage. Progressive crustal thinning favoured mantle upwelling and melting at greater depth, leading to the characteristic alkaline signature (Bixel, 1988; Lago et al., 2004a; Galé, 2005).

7. Tectono-sedimentary evolution of the Permian basins

7.1. Tectonic structure of the basins

Based on the data presented in this work and those published previously, we propose an updated, comprehensive tectono-sedimentary evolution for the Permian basins. This evolution is related to the end of the Variscan orogenic collapse (López-Gómez et al., 2019a, 2021) produced at the beginning of the Alpine cycle.

The Variscan orogen collapse started in late Carboniferous times (late Moscovian) when the Variscan orogeny was still active, and ended in early-middle Permian times (Fernández-Suárez et al., 2000; Ziegler and Stampfli, 2001; López-Sánchez et al., 2015; McCann et al., 2006; Martínez Catalán et al., 2014; López-Gómez et al., 2019a; Dias da Silva et al., 2021). This Permian post-Variscan extensional period extended across the early Permian in the Cantabrian Mountains and reached the middle Permian in the Pyrenees, marking the beginning of the Alpine cycle. This orogenic collapse was moderate and not generalized in the Cantabrian and Pyrenean zones, since these zones were located in the foreland and the transition between the hinterland and foreland of the Variscan orogeny, respectively, where the Variscan crustal thickening was more limited (Pérez-Estaún et al., 1991) (Figs. 1b, 11). Further, extensional collapse gave rise to a horizontal rough cleavage in the Cantabrian Zone, close to some of the large Variscan faults (e.g., León and Liébana faults, Fig. 2) (Pérez-Estaún et al., 1991). This cleavage crosscut the Variscan structures and is compatible with extensional reactivation of associated faults.

Related to this first extensional post-Variscan phase, narrow isolated basins were generated in the Cantabrian range and Pyrenees (Figs. 2, 11). In the Cantabrian Mountains, these basins were controlled by the reactivation of the inherited Variscan and Late Variscan structures, remained active throughout the Cisuralian (López-Gómez et al., 2019a, 2019b) and are filled up to 300 m of sediments (Fig. 5, sections a-g). As the orientation of the main Variscan faults was usually oblique to the lower Permian extensional structures, reactivation of these faults during the Permian was limited. During this stage, the lower Permian basins of eastern AGR of the Cantabrian Mountains, developed on the arcuate Variscan Cantabrian Zone (Figs. 1b, 2), were strongly controlled by: i) *E*-W Variscan thrusts (e.g., Sotres Basin) (Fig. 2, number 1; Fig. 12b), ii)

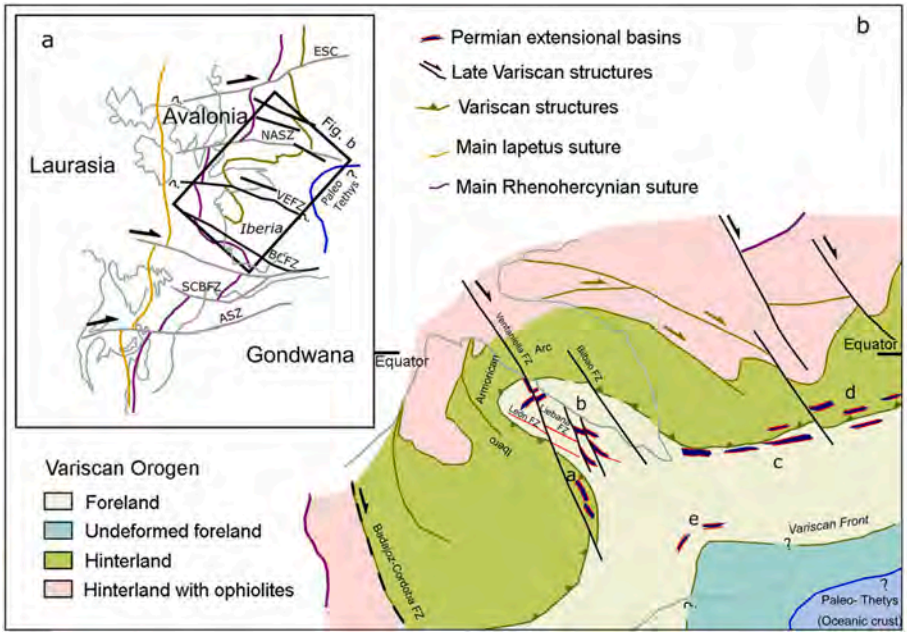

Fig. 11. a) Sketch showing the location of the studied region and the main sutures of Pangea during the early Permian. Legend in the figure is valid for both 1a and 1b. ESZ-Elbe Shear Zone, NASZ- North Armorican Shear Zone, VEZF-Ventaniella Fault Zone, BCFZ-Badajoz-Cordoba Fault Zone, SCBZ-Southern Banks Fault Zone, ASZ-Atlas Shear Zone. b) The Variscan belt structure and its relationship with the narrow elongated Permian basins. Lower Permian structures and basins are related to the Variscan foreland- hinterland limit (see text for details). Lower Permian location of the equator based on Scotese and Langford, (1995).

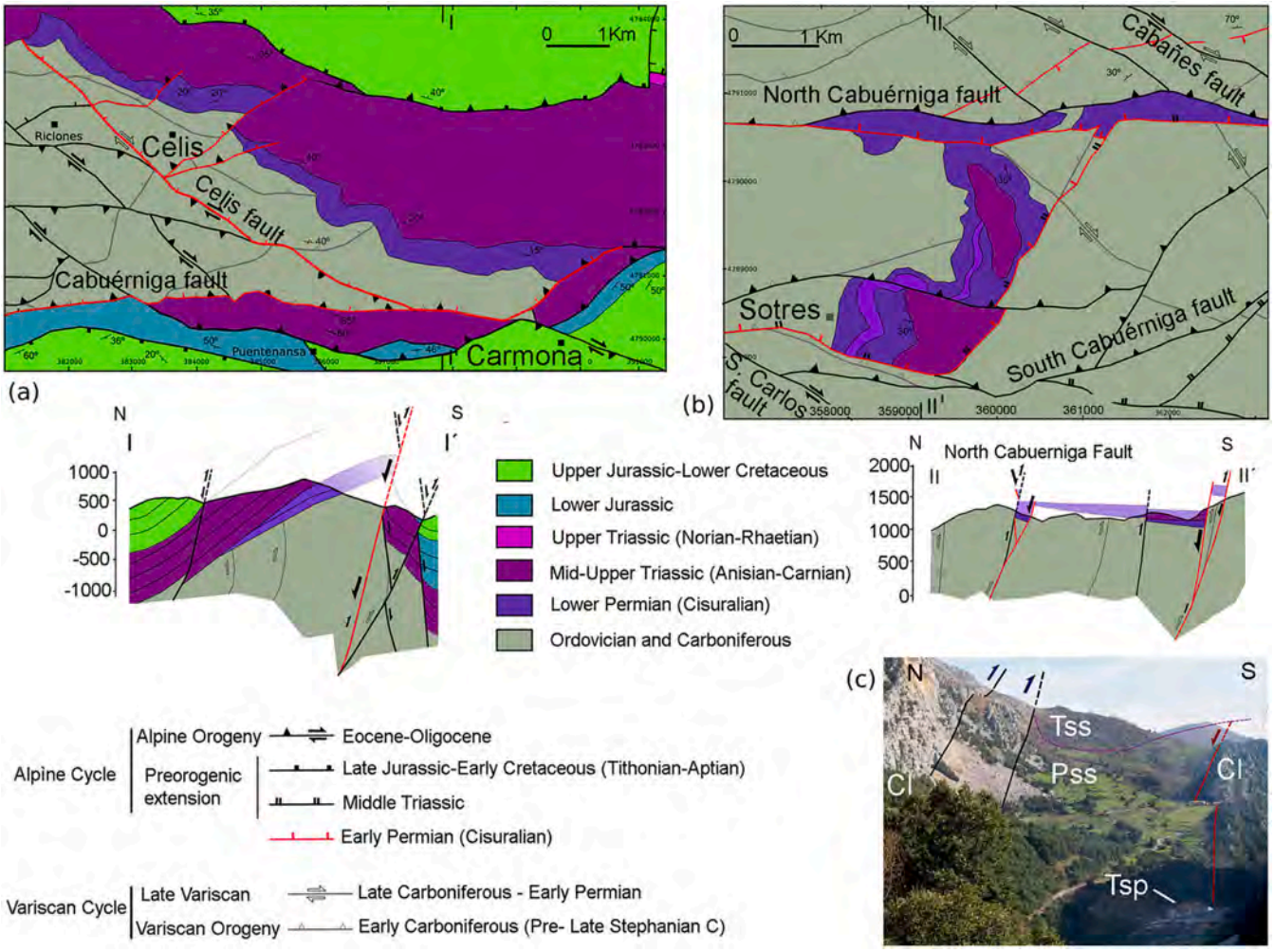

Fig. 12. a) Geological map and cross section of the lower Permian Carmona Basin. Faults reactivated during Permian times appear in red. These faults controlled sedimentation of the Permian deposits and limited the half-grabens. The main structure is the Celis Fault which was a Late Variscan strike-slip fault reactivated during Permian times as a normal fault. The Cabuerniga Fault, which controlled the La Hermida basin, is also observed. The current limits of the sedimentary units were overturned during Alpine compression, which tilted the Permian basin to the north. b) Geological map and cross section of the lower Permian Sotres basin. The faults reactivated during the Permian are indicated in red. These faults controlled Permian deposits and limited the half-graben in the south, while in the north the limit is a fault overturned during the Alpine compression (Cabuerniga fault). c) Photograph showing the Permian La Hermida-Carmona basin. The southern fault is shown, which controlled the sedimentation and northern limit reactivated by the Cabuerniga Alpine fault. At the bottom of the photograph, the Spa can be seen using thermal water (65 °C) from the Permian normal fault. See Fig. 2 for locations of the faults. Cl: Carboniferous limestones; Pss: Permian siltstones and sandstones; Tss Triassic sandstones and siltstones; Tsp: Thermal spa.

NE-SW Variscan thrusts (e.g., La Justa-Aramil and Villaviciosa basins) (Fig. 2, numbers 3, 4) and iii) NW-SE Late Variscan strike-slip faults (e.g., Celís, Peña Labra, Villabona and Peña Sagra basins) (Fig. 2, numbers 2, 5, 6, and 7; Fig. 12a). In the Pyrenees, Permian basins typically trended E-W to NE-SW (Fig. 2), following the Variscan structures of the northern branch of the Ibero-Armorican Arc (Figs. 1b, 11). These basins were elongated, narrow and deep, so that, several hundreds of meters of sediment (up to 700 m) were accumulated in their depocenters (Fig. 5, sections h-m).

To better understand the tectono-sedimentary evolution of the basins, we conducted a detailed study of three well-preserved Permian basins in the Cantabrian Mountains and Pyrenees. These basins are, from W to E: Sotres, Carmona and Somport-Anayet (Fig. 2, numbers 1, 2, 9) and are related to sections c, d and h (Fig. 5). The Sotres Basin extends over an area 10 km long and 2–3 km wide and is now bounded by the Alpine reverse Cabuerniga Fault at its northern border, while the southern border is bounded by the originally normal fault that resulted from a reactivated Variscan thrust. It is here where the thickest section is found, represented by the Sotres Formation (Fig. 12a). To the west, this normal fault is offset southwards, due to the presence of a transfer fault that reactivated a NE-SW Variscan thrust.

The Carmona Basin (Fig. 12b) was related to the reactivation of a NW-SE Late Variscan fault (Celis Fault in Fig. 2, number 2). The maximum size of the Carmona basin and related sub-basins (the Bejes and La Hermida basins) cannot be calculated accurately due to its partial erosion and coverage by Triassic deposits, but we can estimate the basin was 30 km long and 3–4 km wide during the deposition of the Sotres Formation.

Outcrops of the Permian Somport-Anayet basin are among the best preserved in the Pyrenean area and also in all the Pyrenean-Cantabrian belt (Fig. 2 number 9, and Fig. 3), allowing more detailed description here. This NW-SE trending basin extends more than 29 km (Mirouse, 1959) and bears the Midi d'Ossau volcanic complex in its NE part (Figs. 3, 10). At its northern boundary, it is limited by N-100 E direction normal faults, while at its southern border the Permian rocks are unconformably covered by Upper Cretaceous limestones representing the southern limit of the Pyrenean Axial Zone (Fig. 1a). In the easternmost sector of the basin, its southern limit is marked by N-120 E trending

normal faults, reactivated during the Alpine compression. Along the southern part of the Somport-Anayet Basin, both the Permian sediments and the faults that controlled this sedimentation were strongly tilted towards the south, due to fold propagation in the Alpine Gavarnie thrust frontal ramp (Fig. 3c, d). Permian sedimentation in the central part of the Somport-Anayet Basin occurred in relation to WSW-ENE faults, some of which arose from reactivation of Variscan thrusts. The different reactivation ages of these faults prevented the preservation of a complete sedimentary succession of the TU, LRU and URU units in the studied sections.

In the southeastern Pyrenean Axial Zone, normal faults have been described reactivating main Variscan thrusts. These extensional faults trend *E*-W, gently dipping to the North following late-Variscan extension in a N-S to NE-SW direction (Casas et al., 2007). These faults are cut by the Granodiorite of Andorra, dated via U—Pb geochronology as 305 ± 3 Ma (Romer and Soler, 1995), so they are also older than the Permian units examined here. This is because in the Pyrenees, the post-Variscan basins contain both late Carboniferous and Permian sediments. However, it is possible that later movements of these faults or this system, located further south, were those controlling Permian sedimentation in the basins located to the south of the Pyrenean Axial Zone. Saura and Teixell (2006) made a detailed description of Stephano-Permian extensional faults (later inverted during Alpine compression) associated with small basins in the Malpás-Erill Castell and Baró-Estac basins.

7.2. Permian tectono-sedimentary phases

Based on the detailed descriptions of the lithostratigraphic units and their ages, tectonics and magmatism (Figs. 9, 10), three post-Variscan tectono-sedimentary phases (Fig. 13, phases I - III) can be invoked to explain the early-middle Permian sedimentary record of the Pyrenean-Cantabrian orogenic belt. These phases, which are related to extensional reactivation of Variscan thrusts and Late Variscan strike-slip faults, conditioned the appearance or absence of the Permian units and associated magmatism.

In both the Cantabrian Mountains and Pyrenees, lower Permian sedimentation started during the final extensional collapse of the Variscan orogen's foreland (Asselian-Sakmarian in age) and is represented by the Acebal and TU lithostratigraphic units (Fig. 13). In both zones, sedimentation was represented by mid- to distal fluvial deposits with intercalated calc-alkaline volcanic beds. However, in the Cantabrian Mountains, these volcanic intercalations represent a much higher proportion of the sequence than in the Pyrenees. Due to the diachronism of the early Permian extensional event in the eastern Astur-Galaica Region of the Cantabrian Mountains, this first phase of sedimentation is not recorded. Sedimentation during the second Permian extensional tectonic phase (late Artinskian–early Kungurian) is mostly represented by fluvial and lacustrine deposits. In the Pyrenees (LRU), lacustrine deposits and calc-alkaline volcanic beds are intercalated in the fluvial record, while in the Cantabrian Mountains, the lacustrine and its overlying palustrine deposits of the Sotres Formation represent the upper part of a general shallowing sedimentary tendency. Evolution of the sedimentary facies and $\delta^{18}O$ and $\delta^{13}C$ analyses of the studied pedotypes, both in the Cantabrian Mountains and Pyrenees, point to a clear aridification tendency within a monsoon regime for this second tectono-sedimentary phase, which fits in well with the general turnover to a progressive greenhouse phase at the end of the Late Paleozoic Ice Age (LPIA) (Montañez and Poulsen, 2013). The third Permian extensional

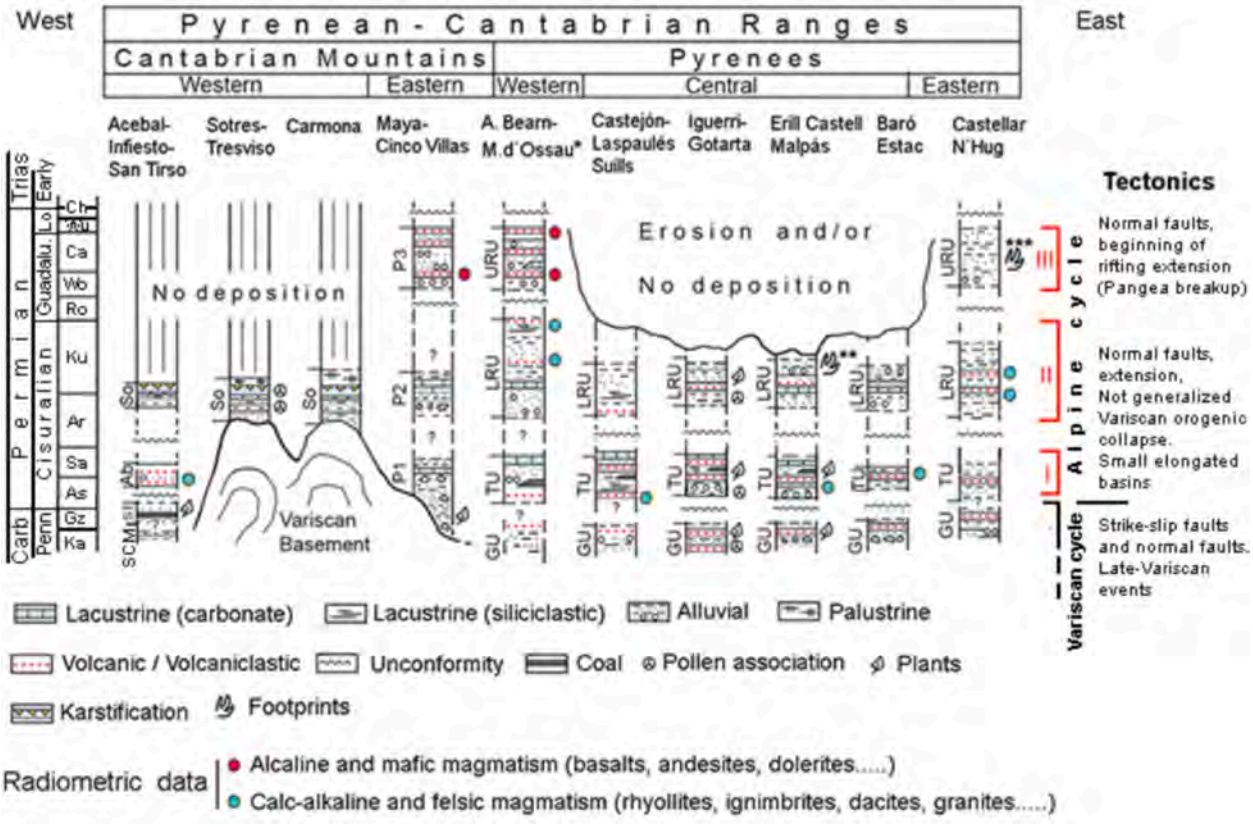

Fig. 13. Sketch of the general distribution of early-middle Permian basins in the Cantabrian Mountains and Pyrenees, showing the three post Variscan extensional tectonic phases of evolution. SCM- Stephanian Cantabrian Mountains. Units: ST- San Tirso, Ab- Acebal, So- Sotres, P1- Permian 1, P2- Permian 2, P3- Permian 3, GU- Gray Unit, TU- Transition Unit, LRU- Lower Red Unit, URU- Upper Red Unit. *Including the surrounding outcrops: Anayet, Sallent de Gallego, Oza and Canal Roya, **Footprints from La Mole d'Amunt (Mujal et al., 2016a), ***Footprints from Noves-La Trava (Mujal et al., 2016b). Radiometric data (U—Pb ages) from: Rodríguez-Méndez et al., 2014 (alkaline and mafic); Valverde-Vaquero et al., 1999 and Pereira et al., 2014 (calc-alkaline and felsic). See text for details.

tectonic phase (Wordian-Capitanian) is mostly represented by fluvial deposits with isolated intercalations of lacustrine and alkaline-mafic volcanic beds in both the eastern Cantabrian Mountains (P3 Unit) and western Pyrenees (URU) (Fig. 13).

8. Discussion. Geodynamic evolution of the Variscan-Alpine transition

8.1. Late-Variscan and early Alpine stages

To the end of the Variscan orogeny (early Gzhelian) the Ibero-Armorican Arc was already very closed in the Cantabrian Zone due to emplacement towards the south of the Picos de Europa Unit (Merino-Tomé et al., 2009) (Fig. 11) and the characteristic thin-skinned deformation of this external zone does not continue in this area. In this context a new stage of thick-skinned deformation started, leading to large dextral strike-slip faults that accommodated the last Variscan shortening (Rodríguez-Fernández and Heredia, 1987). These faults crossed all the Cantabrian Zone with a NW-SE trend and affected all Variscan structures. This episode is know as Late Variscan deformation (Arthaud and Matte, 1975, 1977) and develops in a short time interval, between the early Gzhelian age of the last Variscan thrusts and their *syn*-tectonic sediments, and the early Permian, age of the first syn-extensional pre-orogenic sediments of the Alpine cycle. Related to the Late Varican faults, the sedimentation of the San Tirso Formation occurs in late Gzhelian-early Permian times (López-Gómez et al., 2019a, 2021).

In the geologic literature addressing the beginning of the Alpine cycle in the Pyrenean-Cantabrian orogen, tectono-sedimentary evolution is approached considering the Permian and Triassic records together, and it is common to refer to the Permian-Triassic rifting phase (Hartevelt, 1970; Wagner and Martínez-García, 1982; Lepvrier and Martínez-García, 1990; García-Espina, 1997; Ziegler and Stampfli, 2001; Saura and Teixell, 2006; Gretter et al., 2015; Rodríguez-Méndez et al., 2016; Lloret et al., 2018 and references therein). Based on the virtual absence of lateral continuity of the Permian basins, the scarce age data available for the units described and, therefore, the limited differentiation of the tectonic phases, many authors (e.g., Gretter et al., 2015; Rodríguez-Méndez et al., 2016; Lloret et al., 2018, among others) have suggested that the extension during the beginning of the middle Permian occurred under a dextral transtensional regime related to the first stages of the Pangea break-up, as a global model for the late Variscan and Permian episodes. As a result, some early–middle Permian faults could have occurred as large strike-slip faults related to pull-apart basins. However, there is not definitive evidence of the presence of this type of fault in this tectonic extensional context. They may consist of linked discontinuous traces inferred under Mesozoic sediments, as stated by Saura and Teixell (2006) who, after restoring structural sections, confirmed that Permian sub-basins initially formed as grabens or half-grabens.

Recently, Heredia et al. (2019) and López-Gómez et al. (2019a) proposed a different evolution model for the Permian and Triassic basins, which are separated by a stratigraphic gap of more than 30 Myr in the Cantabrian Mountains (middle Permian to late Middle Triassic), and somewhat less in the Pyrenees (late Permian-Early Triassic). These authors linked the Permian extensional regime to the end of the collapse of the Variscan orogen. Accordingly, after the Variscan orogeny in early Permian times (Cisuralian), the foreland of the Pyrenean-Cantabrian orogen was affected by a slight and not generalized collapse that produced elongated, narrow isolated extensional basins and an associated calk-alkaline to alkaline magmatism (Bixel, 1987; Debon et al., 1996; Gallastegui et al., 1990, 2004). For many authors (Fernández-Suárez et al., 2000; Ziegler and Stampfli, 2001; López-Sánchez et al., 2015; McCann et al., 2006; Martínez Catalán et al., 2014; López-Gómez et al., 2019a; Dias da Silva et al., 2021), the collapse started in the thickened hinterland of the Variscan orogen (Central Iberian Zone, Fig. 1b) in the late Moscovian (ca. 310 Ma), when closure of the Ibero-Armorican Arc started in the Cantabrian Zone with the emplacement of the Bodón-Ponga Unit towards the east (Rodríguez-Fernández and Heredia, 1987, 1988; Heredia, 1998; Gutiérrez-Alonso et al., 2011). This episode has related igneous rocks and is represented by some large normal faults, such as the Allende fault (Marcos, 1973), Vivero fault (López-Sánchez et al., 2015) or the Chandoiro fault (Farias and Marcos, 2019). The collapse reached the slate belt of the Variscan hinterland (West Asturian-Leonese Zone) and the internal part of the Variscan foreland (Cantabrian Zone) in Kasimovian-Gzhelian times (ca. 305–300 Ma), where large extensional continental basins were filled with thick sedimentary continental successions (up to thousands of meters thick). These basins were slightly deformed by the Variscan orogeny and recorded some igneous activity (Merino-Tomé et al., 2017), which also affected the strongly deformed pre-Kasimovian basement (Fernández-Suárez et al., 2000). This extensional collapse is contemporaneous with the development of the last contractional structures in the outermost parts of the Variscan orogen: the emplacement of the Picos de Europa Unit towards the south (Merino-Tomé et al., 2009) and the subsequent late Variscan NO-SE strike-slip faults (Rodríguez-Fernández and Heredia, 1987) causing the main and final closure of the Ibero-Armorican Arc, respectively.

The tectono-sedimentary context for the post-Variscan Permian basins of the Pyrenees and Cantabrian Mountains is similar. In both cases, small elongated basins (few kilometers in scale) were limited by normal faults that formed small grabens or semi-grabens without connection. These basins were generated at the end of the Variscan orogenic collapse, which affected all the Variscan orogenic belt in the early Permian. In the foreland and in the foreland-hinterland boundary of the Variscan orogen, sedimentary and igneous rocks are present (Suárez-Rodríguez, 1988; Gallastegui et al., 1990, 2004; Valverde-Vaquero, 1992), but large outcrops of igneous rocks are only preserved in lower Permian basins (ca. 295–285 Ma) (Fernández-Suárez et al., 2000; Gutiérrez-Alonso et al., 2011; López-Gómez et al., 2021).

Pereira et al. (2014) relate the late Carboniferous-early Permian calc-alkaline magmatism with a subduction-related cycle (Cimmerian cycle), product of the subduction of the Paleotethys (Fig. 11) beneath the Varican belt. This scenario is difficult to reconcile with the data presented here, because this magmatism is distributed throughout the NW Iberian Massif with a similar age and it would be located, in many cases, very far from the possible subduction zone. This far location would imply a flat-slab subduction as it happened in the Andes (Ramos and Folguera, 2009 and references therein) or in the Rocky Mountains (Blakey and Ranney, 2018 and references therein), in which this subduction type would produce arc migration (magmatic arcs with different ages) and a compressive deformation that would propagate across the continent beyond the successive magmatic arcs (García-Sansegundo et al., 2014). Neither of these processes are recorded in this segment of the Variscan orogen. Moreover, Bea et al. (2021) concluded that the overall chemical and isotopic compositions of most Central Iberian Zone granitoids of the Variscan belt (Fig. 1) with late Carboniferous-early Permian age, are different from subduction-related granite rocks. These authors argued that mantle-derived mafic-intermediate rocks in this area, which should best preserve information on the type of melt generation processes, do not preserve arc-related signatures either.

Also, a crustal delamination that led to the formation of juvenile melts during the closure of the Ibero Armorican Arc has been invoked, especially to explain the magmatism developed in the Variscan foreland (Gutiérrez-Alonso et al., 2004, 2011, 2015). In our opinion and also that of other authors (Burg et al., 1994; Ziegler and Stampfli, 2001), in the areas affected by the late Carboniferous-early Permian orogenic collapse, an asthenospheric uplift induced thermal thinning of the mantle-lithosphere and a magmatic inflation of the remnant lithosphere. In both last cases, the extensional reactivation of large and deep Variscan and Late Variscan faults during the orogenic collapse allowed the emplacement of igneous rocks in upper crustal levels and at the surface (Gallastegui et al., 1990).

The formation of small, isolated basins cannot be related to the

generalized extension that occurred at a later stage, during the Triassic, associated with large regional structures. Most of the Permian basins respond mainly to a N-S extension (in the current position of the Iberian Peninsula) that could already be related to the beginning of the stress field generalized during the Triassic extension (Triassic rifting) (Fig. 11). This Permian extensional collapse finished during the end Kungurian (end of early Permian) in the Cantabrian Mountains or even Wordian-Capitanian (middle Permian) in the Pyrenees, and is characterized by a transition from calc-alkaline to alkaline magmatism. This transition can mark a continuous event of extension in the Pangea continental crust, leading initially to crustal melts with calc-alkaline signatures, and evolving to the upper lithospheric mantle partial melting that produced alkaline magmas.

This final middle Permian phase of Variscan orogen collapse, also marks the transition to Triassic rifting (López-Gómez et al., 2019a) (Fig. 13), but this extensional process stopped, at least for about 10 Myr in the Pyrenees and 30 Myr in the Cantabrian Mountains. Then again, in Early (Pyrenees) -Middle Triassic (Cantabrian Mountains) times, the extensional process was reactivated as the result of the beginning of the breakup of Pangea (Lloret et al., 2020) which at this latitude was represented by the opening of the Bay of Biscay. The Bay of Biscay is an eastern branch of the North Atlantic rift that remained active until Early Cretaceous, allowing the separation of the Iberian subplate from the Euroasian plate, although this rifting process also stopped during Early and Middle Jurassic (Boillot et al., 1979). The Triassic rifting started earlier in the Pyrenees because during this time the rift axis must have been close to these ranges, while the present Cantabrian Mountains were located near to the southern edge of this rift, where the extensional process (rift propagation) came later.

Some minor differences can be observed in the tectono-sedimentary characteristics of the early Permian collapse between the Cantabrian Mountains and the Pyrenees: 1) In the Pyrenees, the Permian and Stephanian basins coincide and the lower Permian deposits sometimes rest on the Stephanian deposits in apparent conformity (e.g., Gretter et al., 2015; Lloret et al., 2018). This implies that here, the beginning of the sedimentary record of the Permian extensional basins could be the continuation of the Stephanian basins, while these deposits differ in the Cantabrian Mountains, where they are separated by an angular unconformity. 2) The sedimentary fill in the Permian basins of the Pyrenees is about one thousand meters thick, while in the Cantabrian Mountains only a few hundred meters of sediment fill the basins. This could be because in the Pyrenees, the Permian basins are located near the hinterland of the Variscan orogen (Figs. 1b, 11, 13), where the crust was thicker and therefore the post-orogenic extensional collapse was more relevant. Erosion could also be invoked, related a post-Permian generalized uplift in the Cantabrian Mountains, but the tectonic context in Permian times is always extensional and not generalized, so elevated areas subject to erosion predominate over the sedimentary basins. 3) In the Cantabrian Mountains, the extensional faults that controlled the Permian basins were generally related to reactivations of Variscan faults (thrusts and Late-Variscan strike-slip faults), while in the Pyrenees, reactivation of Variscan structures is not as common. This is probably because in the Pyrenees the Variscan faults are older (pre-Stephanian) and do not usually present a favorable orientation, so they are more difficult to reactivate. By contrast, in the Astur-Galaica Region (Variscan Cantabrian Zone), especially in its easternmost part, the Variscan structures are brittle and younger (Stephanian-Permian) in age (Fig. 11) and can be reactivated more easily. 4) The general characteristics of the sedimentary record and its age are similar both in the Cantabrian Mountains and Pyrenees, although some differences are remarkable. The first is that with the exception of the easternmost area, most Permian sedimentation in the Cantabrian Mountains is recorded in only two units, the Acebal and Sotres formations, while in the Pyrenees it is represented by three formations (TU, LRU and URU) (Fig. 13). In most of the Cantabrian Mountains, sedimentation was interrupted during the Kungurian, and reinitiated again in the Middle Triassic, after a long gap of 30 Myr (López-Gómez et al., 2019a). This interruption was associated with exposure and intense karstification processes affecting most of the Cantabrian area. In the Pyrenees, a new extensional phase developed during the middle Permian, which was affected by intense erosion prior to the beginning of the Early Triassic (Olenekian) sedimentation (Lloret et al., 2020).

8.2. Late-Variscan and early Alpine Western-Central Europe scenario

After the mid to late Carboniferous, oblique convergence between south Laurussia and north Gondwana gave rise to the large European and Mediterranean segment of the Variscan orogeny. The two components of the system started moving apart again through dextral transpressional megashear, involving Europe, North America and the Mediterranean area at the same time (e.g., Arthaud and Matte, 1977; Matte, 1986; Bard, 1997) (Fig. 11a). However, the general NW–SE latest Carboniferous shortening trend continued during the early Permian (Stampfli and Borel, 2002; Muttoni et al., 2009; Martínez-Catalán, 2011; Aubele et al., 2012; Cassinis and Doubinger, 1992; Cassinis et al., 2012; Bachtadse et al., 2018; Elter et al., 2020), although large areas of the hinterland of the arcuate Variscan orogen were already collapsing since the late Carboniferous (late Moscovian). During this orogenic collapse a large number of igneous rocks were distributed throughout the Variscan belt, appearing as volcanic intercalations in the late Carboniferous-Permian basins. As a result, the late Carboniferous paleogeography of Western Europe features large epicontinental seas that range from fully marine to brackish-paralic or evaporitic (Izart and the 343 IGCP working group, 1998, Izart et al., 2003) and developed near to the prograding Variscan orogenic front in the Bashkirian to Gzhelian ages (Águeda et al., 1991; Merino-Tomé et al., 2009; Voldman et al., 2020). In continental areas deformed and thickened by Variscan orogeny, collapse-related basins filled by sediments, mostly alluvial and lacustrine, characterized the Variscan hinterland of Central-Western Europe during the Kasimovian-Gzhelian (up to 6 km thick) and the foreland during the early Permian (up to 2 km thick) (McCann et al., 2006) when the Variscan orogeny had already finished. Extensional collapse migrated from the Variscan hinterland while intramontane basins decreased in size, developing small basins on the distal foreland in Permian times (Fig. 11b). Compared to the late Carboniferous basins, the Permian basins increased in number but the thickness of sedimentary fill decreased, suggesting smoothing of the Variscan chain relief (Vai, 2003).

During the early Permian, most Western and Central European basins were located at the equator or in near-equator areas (Scotese and Langford, 1995). As a result of gradual lower Permian fragmentation, there was extensive rift-related tectonism and associated extensional magmatic activity. Despite differences in both timing and location, the similarity in terms of basin infill (sedimentary and magmatic) between these basins is remarkable (McCann et al., 2006) and general comparisons between basins can be made through precise (radiometric) dating.

The onset of post-Variscan sedimentation was conditioned by the presence of regionally uplifted areas. Wrench-related lithospheric deformation, magmatic inflation of the lithosphere and thermal erosion of the lithospheric mantle could be the joint triggers for the uplift (McCann et al., 2006), which was accompanied by periods of significant magmatic activity. As a result of this paleorelief, the first post-Variscan sediments were deposited in some basins, mostly alluvial in origin, continuously from the latest Carboniferous (Kasimovian-Gzhelian). Other basins started sedimentation during the Asselian or even later (Fig. 14). All these basins, however, experienced significant magmatic activity. Melt generation was probably related to the partial melting of the uppermost asthenosphere and lithospheric thermal boundary layer (Ziegler, 1990), the most voluminous concentrations occurring in the North German Basin (Benek et al., 1996) dated at ca. 297–302 Ma (Breitkreuz and Kennedy, 1999). The latest Carboniferous to earliest Permian period coincided with an intense negative deviation of the

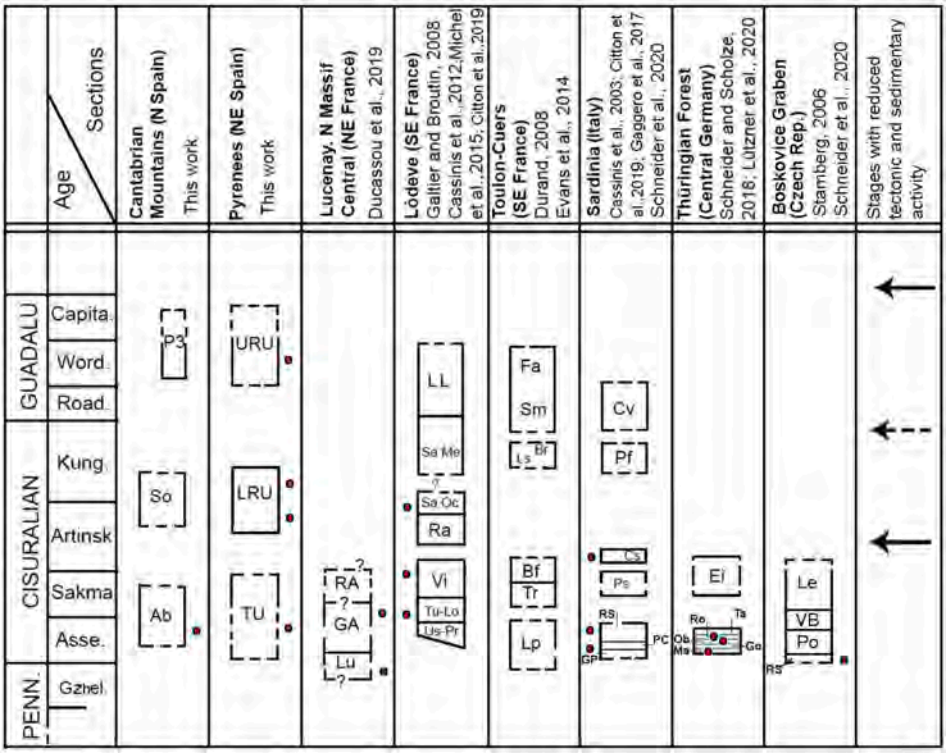

Fig. 14. Schematic comparison of the post-Variscan extensional tectonic phases recorded in the study area and representative coeval basins in Western and Central Europe. Arrows indicate common stages of prolonged hiatuses without sedimentation or reduced subsidence and accumulation of sediments. Units- Ab: Acebal; So: Sotres; P3: Permian 3; TU: Transition Unit; LRU: Lower Red Unit; URU: Upper Red Unit; Lu: Lucenay; GA: Autunian Gray; RA: Red Autunian; Uselas; Pr: St. Prirat; Tu: Tuileres; Lo: Loiras; Vi: Viola; Ra: Rebajac; Sa - Oc: Salagou (Fm) - Octon (Mb); LL: La Lieude (Fm); Sa – Me: Salagou (Fm) - Merifons (Mb); Lp: Les Pellegrins; Tr: Transy; Bf: Bron; Ls: Les Salettes; Br: Calc. du Bau Rouge; Sm: St. Mandrier; Fa: Fabregas; GP: Guarda Pisano; PC: Punta Lu Caparoni; RS: Rio Su Luda; Ps: Pedru Siligu; Cs: Casa Satta Ignimbrite; Pf: Porto Ferro; CV: Cala del Vino; Ma: Manebach; Go: Goldlauter; Ob: Oberode; Ro: Rotterode; Ta: Tacenbach; Ei: Eisenach; RO: Rosice-Oslavany (Fm); Po: Podochov (Fm); VB: Veverská-Bitýska (Fm); and Le: Letovice (Fm). (Citton et al., 2019; Ducassou et al., 2019; Evans et al., 2014; Gaggero et al., 2017; Lützner et al., 2020; Michel et al., 2015)

atmospheric CO_2 concentration curve (Montañez et al., 2016), witnessing a late and intense cold episode of the Late Paleozoic Ice Age.

During the Artinskian, the tectonic activity of Western and Central European basins experienced a period of change. Sedimentation decreased during the early Artinskian, and a period of general tectonic quiescence in most of these basins resulted in hiatuses in sedimentation (Fig. 14). The late Artinskian-Kungurian period was one of renewed reactivation in most basins, inducing the accumulation of considerable sediment thicknesses. This period, combined with a general decrease in glacial frequency, aerial extent of vegetation (Montañez and Poulsen, 2013) and a consolidated trend towards semiarid and arid conditions in the European basins, may have coincided with the end of the Late Paleozoic Ice Age (Tabor and Montañez, 2004; DiMichele et al., 2008).

Some Western European basins occupying the foreland of the Variscan orogenic belt (e.g., Cantabrian Mountains basins) underwent prolonged exposure again at the end of the Kungurian (Fig. 14). However, this period of time featured different tectono-sedimentary scenarios, as basins located adjacent to, or to the north of the Variscan deformation front experienced subsidence related to thrust loading of the crust and a more continuous form of sedimentation (McCann et al., 2006). In most basins, the Wordian-Capitanian (end Guadalupian) represented the end of this sedimentation phase.

During the early-middle Permian, similar extensional post-Variscan tectono-sedimentary pulses were recorded across the Pyrenean-Cantabrian orogen. These pulses were related to the geodynamic response of the asthenosphere and lithosphere to the crustal instability that was to follow the Variscan orogeny. The Western and Central Europe basins formed within the Variscan hinterland experienced broadly the same pulses. Differences between the sedimentary and volcano-sedimentary infill and associated magmatic activity were probably linked to the relative position of the basins in the Variscan orogenic belt, with different thickening and melting levels in the crust.

9. Conclusions

The Post-Variscan evolution of the Pyrenean-Cantabrian orogenic belt is related to a lower Permian extensional regime, associated with the final collapse of the Variscan orogen, which triggered the beginning of the Alpine cycle. For the first time, a multi-disciplinary study of the stratigraphy, sedimentology, paleosols, tectonics and volcanism of well-dated lower-middle Permian units confirms the similar post-Variscan geodynamic evolution across the entire Pyrenean-Cantabrian belt.

The collapse of the Variscan orogen started in the hinterland in late Carboniferous times (late Moscovian), when the Variscan orogeny was still active in the external foreland, and reaching the all foreland in Permian times, when the Variscan orogeny had already ended. The orogenic collapse finished in the Cantabrian Mountains in early Permian times and in the middle Permian in the Pyrenees.

The extensional processes related to the Variscan orogen collapse were not generalized, and gave rise to larger intramontane basins in the hinterland-foreland boundary during the late Carboniferous (Kasimovian-Gzhelian) than in the foreland, where smaller, thinner, elongated isolated basins developed during the early and middle Permian.

The extensional reactivation of large and deep Variscan and Late Variscan faults during the orogenic collapse allowed the emplacement of late- and post-Variscan igneous rocks in upper crustal levels or on the surface. These late Carboniferous-middle Permian igneous rocks can be related to an asthenospheric uplift and crustal thinning related to this collapse, which was higher in the thickened hinterland of the Variscan orogen, where the igneous rocks of this age were more abundant.

The first phase (Asselian-Sakmarian) comprises alluvial sediments and calc-alkaline volcanic rocks. The second phase (late Artinskian-early Kungurian) is represented by alluvial, lacustrine and palustrine sediments with intercalations of calc-alkaline volcanic beds, with a clear aridification tendency. The third phase (Wordian-Capitanian) was not deposited in the Cantabrian Mountains, and caused significant erosion in the Pyrenees. It consists of alluvial deposits with intercalations of alkaline and mafic beds. This last Permian extensional phase marks the transition to a rifting stage, which doesn't begin until Early-Middle Triassic times, indicating a pause in the extensional process of at least 10 Myr in the Pyrenees and for about 30 Myr in the Cantabrian Mountains. The Triassic rifting was related to the opening of the Bay of Biscay,

an eastern branch of the North Atlantic rifting, which represents the Pangea break-up at these paleolatitudes.

Based on the evolution of near-equator post-Variscan or early Alpine pre-orogenic basins in Europe, we infer similarities between the geodynamic and climate evolution of the Pyrenean-Cantabrian basins and those formed within Western and Central Europe during the early-middle Permian. Common features include prolonged hiatuses in sedimentation, magmatic activity, related extensional faulting and stages of increased subsidence and accumulation of the sedimentary record, as well as a progressive climate aridification. Our comparison also highlights evolutionary differences between basins likely controlled by their location within the Variscan orogenic belt.

Declaration of Competing Interest

This article is based on an original work, both in its text and in the figures, and is sent to be published in Global and Planetary Change with the consent of all co-authors.

There are not conflicts of interest.

Acknowledgements

The authors thank Dr. Agustín Pieren (Universidad Complutense de Madrid, Spain) for the data of La Camocha Mine and Ana Burton for editorial assistance. The authors thank the detailed review and the interesting comments from the reviewers Ícaro Dias da Silva (Universidade de Lisboa), Antonio Teixell (Universitàt Autònoma de Barcelona), Francisco Pereira (Universidade de Évora) and an anonymous reviewer. Funds were provided by projects PGC2018-098272-B-100 and CGL2015-70970-P "FALPINO" (Spanish Ministry of Science, Innovation and Universities).

References

Abels, H.A., Sbdul Aziz, H., Calvo, J.P., Tuenter, E., 2004. Shallow lacustrine carbonate microfacies document orbitally paced lake-level history in the Miocene Teruel Basin (North-East Spain). Sedimentology 56 (2), 399–420.

Águeda, J.A., Bahamonde, J.R., Barba, F.J., Barba, P., Colmenero, J.R., Fernández, L.P., Salvador, C.I., Vera, C., 1991. Depositional environments in Westphalian coal-bearing successions of the Cantabrian Mountains, North West Spain. Bull. Soc. Geol. Fr. 162, 325–333.

Alonso, J.A., Pulgar, J.A., García Ramos, J.C., Barba, P., 1996. Tertiary basins and Alpine tectonics in the Cantabrian Mountains (NW Spain). In: Friend, P.F., Dabrio, C.J. (Eds.), Tertiary Basins of Spain. University Press, Cambridge, pp. 214–227.

Alonso-Zarza, A.M., Wright, P.V., 2010. Palustrine carbonates. Carbonates in Continental Settings: facies, environments and processes. In: Developments in Sedimentology, 61. Elsevier, Amsterdam, pp. 225–267.

Alonso-Zarza, A.M., Meléndez, A., Martín-García, R., Herrero, M.J., Martín-Pérez, A., 2012. Discriminating between tectonism and climate signatures in palustrine deposits: lessons from the Miocene of the Teruel Graben, NE Spain. Earth Sci. Rev. 113, 141–160.

Anderweg, B., 2002. Cenozoic Tectonic Evolution of the Iberian Peninsula, Causes and Effects of Changing the Stress Field. PhD Thesis. Vrie University, Amsterdam, 178 p.

Arguden, A.T.F., Rodolfo, K.S., 1990. Sedimentologic and dynamic differences between hot and cold laharic debris flows of Mayon Volcano, Philippines. Geol. Soc. Am. Bull. 102, 865–876.

Arranz, E., 1997. Petrología del Macizo Granítico de La Maladeta (Huesca-Lérida): Estructura, Mineralogía, Petrología y Petrogénesis. Ph.D Thesis. Universidad de Zaragoza, 338p.

Arthaud, F., Matte, P., 1975. Les decrochements tardi-hercyniens du sud-ouest de l'Europe, geometrie et essai de reconstitution des conditions de la deformation. Tectonophysics 25, 139–171.

Arthaud, F., Matte, P., 1977. Late Paleozoic strike-slip faulting in southern Europe and northern Africa: result of a right-lateral shear zone between the Appalachians and the Urals. Geol. Soc. Am. Bull. 88, 1305–1320.

Aubele, K., Bachtadse, V., Muttoni, G., Ronchi, A., Durand, M., 2012. A paleomagnetic study of Permian and Triassic rocks from the Toulon-Cuers Basin, SE France: evidence for intra-Pangaea block rotations in the Permian. Tectonics 31, 1–14.

Bachtadse, V., Aubele, K., Muttoni, G., Ronchi, A., Kirscher, U., Kent, D.V., 2018. New early Permian paleopoles from Sardinia confirm intra-Pangaea mobility. Tectonophysics 749, 21–34.

Bard, J.-P., 1997. Demembrement ante-mesozoique de la chaine varisque d'Europe occidentale et d'Afrique du Nord: role essentiel des grands decrochements transpressifs dextres accompagnant la rotation-translation horaire de l'Afrique durant le Stephanien. C. R. Acad. Sci. Paris (IIa) 324, 693–704.

Barnolas, A., Pujalte, V., 2004. La Cordillera Pirenaica. In: Vera, J.A. (Ed.), Geología de España. IGME-SGE, Madrid, pp. 233–343.

Barnolas, A., Larrasoaña, J.C., Pujalte, V., Schmitz, B., Sierro, F.J., Mata, M.P., van den Berg, B.C.J., Pérez-Asensio, J.N., Salazar, A., Salvany, J.M., Ledesma, S., García-Castellanos, D., Civis, J., Cunha, P., 2019. Alpine Foreland basins. In: Quesada, C., Oliveira, J.T. (Eds.), The Geology of Iberia: A Geodynamic Approach, vol. 4, pp. 7–59. Cenozoic Basins.

Bea, F., Gallastegui, G., Montero, P., Scarrow, J., Cuesta, A., González-Menéndez, L., 2021. Contrasting high-Mg, high-K rocks in Central Iberia: the appinite-vaugnerite conundrum and their (non-existent) relation with arc magmatism. J. Iber. Geol. 47, 235–261.

Benek, R., Kramer, W., McCann, T., Scheck, M., Negendank, J.F.W., Korich, D., Huebscher, H.-D., Baye, U., 1996. Permo-Carboniferous magmatism of the Northeast German Basin. Tectonophysics 266, 379–404.

Berra, F., Felletti, F., Tessarollo, A., 2019. Oncoids and groundwater calcrete in a continental siliciclastic succession in a fault-controlled basin (Early Permian, Northern Italy). Facies 65 (4), 38.

Bixel, F., 1984. Le magmatism stéphano-permien des Pyrénées. University of Toulouse, Toulouse, France. Unpublished.

Bixel, F., 1987. Le Volcanisme Stéphano-Permien des Pyrénées: pétrographie, minéralogie, géochimie. Cuadernos de Geología Ibérica 11, 41–55.

Bixel, F., 1988. Le volcanisme stéphano-permien des Pyrénées atlantiques. Bull Centres Rech Explor-Prod Elf-Aquitanie 12 (2), 661–706.

Blakey, R.C., Ranney, W.D., 2018. Flat-Slab Subduction, the Laramide Orogeny, Uplift of the Colorado Plateau and Rocky Mountains: Paleocene and Eocene: Ca. 65–35 Ma. In: Ancient Landscapes of Western North America. Springer, Cham. https://doi.org/10.1007/978-3-319-59636-5_9.

Boillot, G., Dupeuble, P.A., Malod, J., 1979. Subduction and Tectonics on the continental margin off northern Spain. Mar. Geol. 32, 53–70.

Bonin, B., 1990. From orogenic to anorogenic settings: evolution of granitoid suits after a major orogenesis. Geol. J. 25, 261–270.

Breitkreuz, C., Kennedy, A., 1999. Magmatic flare-up at the Carboniferous/Permian boundary in the NE German Basin revealed by SHRIMP zircon ages. Tectonophysics 302 (3–4), 307–326.

Breitkreuz, C., Cortesogno, L., Gaggero, L., 2001. Crystal-rich mass flow deposits related to the eruption of a sublacustrine silicic cryptodome (Early Permian Collio Basin, Italian Alps). J. Volcanol. Geotherm. Res. 114, 373–390.

Briqueu, L., Innocent, C., 1993. U/Pb zircon dating and Sr and Nd isotope characteristics of Permian volcanism in the Western Pyrenees: the Ossau and Anayet Massif. Comptes Rendus Academie Sciences Paris Ser II 316 (5), 623–628.

Broutin, J., Gisbert, J., 1985. Entorno paleoclimático y ambiental de la flora stephano-autuniense del Pirineo catalán. In: Compte rendux Dixième International de Stratigraphie et de Géologie du Carbonifère, pp. 53–66.

Broutin, J., Cabanis, B., Chateauneuf, J.J., Deroin, J.P., 1994. Evolution biostratigraphique, magmatique et tectonique du domaine paleotethysien occidental (SW de l'Europe); implications paleogeographiques au Permien inferieur. Bulletin de la Société Géologique de France 165 (2), 163–179.

Burg, J.P., Van Den Driesche, J., Brun, J.P., 1994. Syn- to post-thickening extension in the Variscan belt of western Europe: modes and structural consequences. Géol. Fr. 3, 33–51.

Burns, C.F., Mountney, N.P., Hodgson, D.M., 2017. Anatomy and dimensions of fluvial crevasse-splay deposits: examples from the Cretaceous Castlegate Sandstone and Neslen Formation, Uthah, USA. Sediment. Geol. 351, 21–35.

Cámara, P., 1997. The Basque-Cantabrian basin's Mesozoic tectono-sedimentary evolution. Mémoires Société Geologique de France 171, 187–191.

Cámara, P., 2017. Salt and Strike-Slip Tectonics as Main Drivers in the Structural Evolution of the Basque-Cantabrian Basin, Spain. In: Soto, J.I., Flinch, J.F., Tari, G. (Eds.), Permo-Triassic Salt Provinces of Europe, North Africa and the Atlantic Margings. Elsevier, pp. 371–393.

Capote, R., Muñoz, J.A., Simón, J.L., Liesa, C.L., Arlegui, L.E., 2002. Alpine tectonics I: The Alpine Sytem north of the Betic Cordillera. In: Gibbons, W., Moreno, T. (Eds.), Geology of Spain. Geology of Spain. Geological Society, London, pp. 385–397.

Carballo, A., Fernández, M., Jimenez-Munt, I., Torne, M., Vergés, J., Melchiorre, M., Pedreira, D., Alfonso, J.C., García-Castellanos, D., Diez, J., Villaseñor, A., Pulgar, J., Quintana, L., 2015. From the North-Iberia Margin to the Alborán Basin: a lithosphere geo-transect crossing the Iberia Plate. Tectonophysics 663, 399–418.

Casas, J.M., Fernández, O., Domingo, F., 2007. Carboniferous normal faults in the Eastern Pyrenees: evidences and age constrains of syn-orogenic Variscan extension. Geodin. Acta 20 (6), 385–392.

Cassinis, G., Doubinger, J., 1992. Artinskian to Ufimian palynomorph assemblages from the central Southern Alps, Italy, and their regional stratigraphic implications. In: Presented at the Contribution to Eurasian Geology. Intern. Congress on the Permian System of the World, pp. 9–18.

Cassinis, G., Perotti, C.R., Ronchi, A., 2012. Permian continental basins in the Southern Alps (Italy) and peri-Mediterranean correlations. Int. J. Earth Sci. (Geologische Rundschau) 101, 129–157.

Choukroune, P., 1992. Tectonic evolution of the Pyrenees. Annu. Rev. Earth Planet. Sci. 20 (1), 143–158.

Choukroune, P., Roure, F., Pinet, B., Pyrenees Team, E.C.O.R.S., 1990. Main results of the ECORS Pyrenees profile. Tectonophysics 173, 411–423.

Citton, P., Ronchi, A., Maganuco, S., Caratelli, M., Nicosia, U., Sacchi, E., Romano, M., 2019. First tetrapod footprints from the Permian of Sardinia and their palaeontological and stratigraphical significance. Geol. J. 54 (4), 2084–2098.

Colmenero, J.R., Fernández, L.P., Moreno, C., Bahamonde, J.R., Barba, P., Heredia, N., González-Martín, F., 2002. Carboniferous. In: Gibbons, W., Moreno, T. (Eds.), Geology of Spain. The Geological Society, London, pp. 93–116.

Colombi, C.E., Limarino, C.O., Alcober, O.A., 2017. Allogenic controls on the fluvial architecture and fossil preservation of the Upper Triassic Ischigualasto Formation, NW Argentina. Sediment. Geol. 362, 1–16.
Cortesogno, L., Cassinis, G., Dallagiovanna, G., Gaggero, L., Oggiano, G., Ronchi, A., Seno, S., Vanossi, M., 1998. The Variscan post-variscan volcanism in Late Carboniferous-Permian Sequences of Ligurian Alps, Southern Alps and Sardinia. Lithos 45, 305–328.
Dalloni, M., 1930. Étude géologique des Pyrénées catalanes. In: Anales Faculté des Sciences de Marseille XXVI, 3, pp. 1–373.
De Haas, T., Van Den Berg, W., Braat, L., Kleinhans, M.G., 2016. Autogenic avulsión, Channelization and Back filling dynamics of debris-flow fans. Sedimentology 63, 1596–1619.
Debon, F., Zimmermann, J.L., 1993. Mafic dykes from some plutons of the western Pyrenean Axial Zone (France, Spain): markers of the transition from late-Hercynian to early-Alpine events. Schweiz. Mineral. Petrogr. Mitt. 73 (3), 421–433.
Debon, F., Enrique, P., Autran, A., Barnolas, A., Besson, M., Bixel, F., Bouchez, J.L., Briqueu, L., Cabaniss, B., Calvet, M., Carreras, J., Centène, A., Charlet, J.M., Charvet, J., Cirès, J., Clin, M., Cocherie, A., Dagallier, G., Dahmani, A., Debat, P., Debon, F., Driouch, Y., Ferrer-Modolell, A., Fonteilles, M., Francois, J.M., García-Sansegundo, J., Gleizes, G., Guitard, G., Inocent, C., Lapierre, H., Laumonier, B., Le Fur-Balouet, S., Leterrier, J., Liesa, M., Martí, J., Mercier, A., Morales, V., Muñoz, J. A., Navidad, M., Palau, J., Pesquera, A., Poblet, J., Pouit, G., Pouget, P., Reche, J., Roux, L., Soler, A., Vaquer, R., Wickham, S.M., 1996. Magmatisme Hercynien. In: Barnolas, A., Chiron, J.C. (Eds.), Synthèse Géologique et Géophysique des Pyrénées. Bureau de Recherches Géologiques et Minières-Instituto Geológico y Minero de España, Orléans-Madrid, pp. 361–500.
Denèle, Y., Paquette, J.-L., Olivier, P., Barbey, P., 2012. Permian granites in the Pyrenees: the Aya pluton (Basque Country). Terra Nova 24, 105–113.
Denèle, Y., Laumonier, B., Paquette, J.-L., Olivier, P., Gleizes, G., Barbey, P., 2014. Timing of granite emplacement, crustal flow and gneiss dome formation in the Variscan segment of the Pyrenees. Geol. Soc. Lond. Spec. Publ. 405, 265–287.
Déramond, J., Graham, R.H., Hossack, J.R., Baby, P., Crouzet, G., 1985. Nouveau modèle de la Chaîne des Pyrénées. Comptes Rendus de l' Académie des Sciences, Série II, Sciences de la Terre et des Planètes 301 (16), 1213–1216.
Deroin, J.P., Bonin, B., 2003. Late variscan tectonomagmatic activity in Western Europe and surrounding areas: the Mid-Permian Episode. Boll. Soc. Geol. It. 2, 169–184. Volume speciale.
Dewey, J.F., Helman, M.L., Turco, E., Hutton, D.H.L., Knott, S.D., 1989. Kinematics of the western Mediterranean. In: Coward, M.P., Dietrch, D., Park, R.G. (Eds.), Alpine Tectonics, Geological Society, London, Special Publications, vol. 45, pp. 265–283.
Dias da Silva, Í., González Clavijo, E., Díez-Montes, A., 2021. The collapse of the Variscan belt: a Variscan lateral extrusion thin-skinned structure in NW Iberia. Int. Geol. Rev. 63, 659–695. https://doi.org/10.1080/00206814.2020.1719544.
DiMichele, W.A., Kerp, H., Tabor, N.J., Looy, C.V., 2008. The so-called "Paleophytic–Mesophytic" transition in equatorial Pangea - Multiple biomes and vegetational tracking of climate change through geological time. Palaeogeogr. Palaeoclimatol. Palaeoecol. 268, 152–163.
Ducassou, C., Mercuzot, M., Bourquin, S., Rossignol, C., Pellenard, P., Beccaletto, L., et al., 2019. Sedimentology and U-Pb dating of Carboniferous to Permian continental series of the northern Massif Central (France): local paaeogeographic evolution and larger scale correlations. Palaeogeogr. Palaeoclimatol. Palaeoecol. 533, 109228. https://doi.org/10.1016/j.palaeo.2019.06.001.
Elter, F.M., Gaggero, L., Mantovani, F., Pandeli, E., Costamagna, L.G., 2020. The Atlas-East Variscan -Elbe shear system and its role in the formation of the pull-apart Late Palaeozoic basins. Int. J. Earth Sci. 109, 739–760. https://doi.org/10.1007/s00531-020-01830-y.
Evans, N.G., Gleizes, G., Leblanc, D., Bouchez, J.L., 1998. Syntectonic emplacement of the Maladeta granite (Pyrenees) deduced from relationships between Hercynian deformation and contact metamorphism. J. Geol. Soc. 155, 209–216.
Evans, M.E., Pavlov, V.E., Veselovskiy, R.V., Fetisova, A.M., 2014. Late Permian paleomagnetic results from the Lodève, Le Luc, and Bas-Argens Basins (southern France): magnetostratigraphy and geomagnetic field morphology. Phys. Earth Planet. Inter. 237, 18–24.
Farias, P., Marcos, A., 2019. Geodynamic evolution of the San Vitero basin, a foreland-type basin developed in the hinterland of the Variscan Orogen (Zamora, NW Spain). J. Iber. Geol. 45, 529–551.
Fernández-Suárez, J., Dunning, G.R., Jenner, G.A., Gutiérrez-Alonso, G., 2000. Variscan collisional magmatism and deformation in NW Iberia: constrains from U-Pb geochronology and granitoids. J. Geol. Soc. Lond. 157, 565–576.
Fernández-Viejo, G., Gallastegui, J., Pulgar, J.A., Gallart, J., 2011. The MARCONI reflection seismic data: a view into the Eastern part of the Bay of Biscay. Tectonophysics 508, 43–41.
Fillon, C., Pedreira, D., Van der Beek, P.A., Husimans, R.S., Barbero, L., Pulgar, J.A., 2016. Alpine exhumation of the central Cantabrian Mountains, northwest Spain. Tectonics 35 (2), 339–356.
Frostick, L.E., Reid, I., 1986. Evolution and sedimentary character of lake deltas fed by ephemeral rivers in the Turkana basin, northern Kenia. In: Frostick, L.E., Renaut, R. W., Reid, I., Tiercelin, J.-J. (Eds.), Sedimentation in the African Rifts, Geological Society Special Publication, vol. 25, pp. 113–125.
Gaggero, L., Gretter, N., Langone, A., Ronchi, A., 2017. U–Pb geochronology and geochemistry of late Palaeozoic volcanism in Sardinia (southern Variscides). Geosci. Front. 8, 1263–1284.
Galé, C., 2005. Evolución Geoquímica, Petrogenética y de Condiciones Geodinámicas de los Magamatismos Pérmicos en los Sectores Central y Occidental del Pirineo. Ph.D Thesis. Universidad de Zaragoza, Zaragoza, p. 457. Unpublished.
Gallastegui, G., Heredia, N., Rodríguez-Fernández, L.R., Cuesta, A., 1990. El stock de Peña Prieta en el contexto del magmatismo de la Unidad del Pisuerga-Carrión (Zona Cantábrica, N de España). Cadernos Laboratorio Xeolóxico Laxe 15, 203–217.
Gallastegui, J., Pulgar, J.A., Gallart, J., 2002. Initiation of an active margin at the North Iberian continent ocean transition. Tectonics 21, 1501–1514.
Gallastegui, G., Suárez, O., Cuesta, A., 2004. Zona Cantábrica: Magmatismo. In: Vera, J. A. (Ed.), Geología de España. SGE-IGME, Madrid, pp. 47–49.
Gand, G., Kerp, H., Parsons, C., Martínez-García, E., 1997. Palaeoenvironmental and stratigraphic aspects of the discovery of animal traces and plant remains in Spanish Permian red beds (Peña Sagra, Cantabrian Mountains, Spain). Geobios 30, 295–318.
García-Espina, R., 1997. La Estructura y Evolución Tectonoestratigráfica del Borde Occidental de la Cuenca Vasco-Cantábrica (Cordillera Cantábrica, NO de España). Tesis Doctoral. Universidad de Oviedo, 230 p. Unpublished.
García-Mondejar, J., 1989. Strike-slip subsidenceof the Basque-Cantabrian Basin of Northern Spain and its relationship to Aptian-Albian opening of the Bay of Biscay. In: Tankard, A.J., Balkwill, H.R. (Eds.), Extensional Tectonics and Stratigraphy of the North Atlantic Margins, 46. American Association of Petroleum Geologists, Memoir, pp. 395–409.
García-Sansegundo, J., Poblet, J., Alonso, J.L., Clariana, P., 2011. Hinterland-foreland zonation of the Variscan orogen in the Central Pyrenees: comparison with the northern part of the Iberian Variscan Massif. Geol. Soc. Lond. Spec. Publ. 349, 169–184.
García-Sansegundo, J., Farias, P., Heredia, N., Gallastegui, G., Charrier, R., Rubio-Ordóñez, A., Cuesta, A., 2014. Structure of the Andean Palaeozoic basement in the Chilean coast at 31° 30' S: Geodynamic evolution of a subduction margin. J. Iber. Geol. 40 (2), 293–308.
Gascón-Cuello, F., Gisbert, J., 1987. La evolución climatica del Stephaniense, Pérmico y Buntsandstein del Pirineo Catalán en base al estudio de paleosuelos. Cuadernos de Geología Ibérica 11, 97–114.
Gil-Imaz, A., Lago, M., Galé, C., Pueyo-Anchuela, O., Ubide, T., Tierz, P., Oliva-Urcia, B., 2012. The Permian mafic dyke swarm of the Panticosa pluton (Pyrenean Axial Zone, Spain): simultaneous emplacement with the late-Variscan extension. J. Struct. Geol. 42, 171–183. https://doi.org/10.1016/j.jsg.2012.05.008.
Gisbert, J., 1981. Estudio Geológico–Petrológico del Estefaniense-Pérmico de la Sierra del Cadí (Pirineo de Lérida): Diagénesis y Sedimentología. Ph.D. Thesis. University of Zaragoza, Spain. Unpublished.
Gisbert, J., 1983. El Pérmico de los Pirineos españoles. In: Martínez García, E. (Ed.), Carbonífero y Pérmico de España. Ministerio de Industria y Energía, Madrid, pp. 405–420.
Gretter, N., Ronchi, N., López-Gómez, J., Arche, A., De la Horra, R., Barrenechea, J., Lago, M., 2015. The Late Paleozoic-Early Mesozoic from the Catalan Pyrenees (Spain): 60 My of environmental evolution in the frame of the western peri-Tethyan palaeogeography. Earth Sci. Rev. 150, 679–708.
Gretter, N., De la Horra, R., Lloret, J., Arche, A., Ronchi, A., López-Gómez, J., Barrenechea, J.F., 2019. The initial (Tectonic) Rifting Phase. In: Quesada, C., Oliveira, J. (Eds.), The Geology of Iberia: A Geodynamic Approach. Volume 3: The Alpine Cycle. Regional Geology Reviews. Springer, Heidelberg, pp. 33–34.
Gulliford, A.R., Flint, S.S., Hodgson, D.M., 2017. Crevasse splay processes and deposits in an ancient distributive fluvial system: the lower Beaufort Group, South Africa. Sediment. Geol. 358, 1–18.
Gutiérrez-Alonso, G., Fernández-Suárez, J., Weil, A.B., 2004. Orocline triggered litospheric delamination. Geol. Soc. Am. Spec. Pap. 383, 121–130.
Gutiérrez-Alonso, G., Fernández-Suárez, J., Jeffries, T.F., Johnson, S.T., Pastor-Galán, D., Murphy, J.B., Franco, M.P., Gonzalo, J.C., 2011. Diachronous post-orogenic magmatism within a developing orocline in Iberia, European Variscides. Tectonics 30 (5). https://doi.org/10.1029/2010TC002845. TC5008.
Gutiérrez-Alonso, G., Collins, A.S., Fernández-Suárez, J., Pastor-Galán, D., González-Clavijo, E., Jourdan, F., Weil, A.B., Johnston, S.T., 2015. Dating of lithospheric buckling: 40Ar/39Ar ages of syn-orocline strike–slip shear zones in northwestern Iberia. Tectonophysics 643, 44–54. https://doi.org/10.1016/j.tecto.2014.12.009.
Hartevelt, J.J.A., 1970. Geology of the upper Segre and Valira valleys, central Pyrenees, Andorra/Spain. Leidse. Geol. Meded. 45, 349–354.
Heredia, N., 1998. Los cabalgamientos del sector suroriental de las Unidades del Ponga y de la Cuenca Carbonífera Central (Zona Cantábrica, NO de España). Trab. Geol. 20, 53–127.
Heredia, N., Martín-González, F., Suárez-Rodríguez, A., 2019. The Variscan Heritage. In: Quesada, C., Oliveira, J. (Eds.), The Geology of Iberia: A Geodynamic Approach. Volume 3: The Alpine Cycle. Regional Geology Reviews. Springer, Heidelberg, pp. 34–36.
Innocent, C., Briqueu, L., Cabanis, B., 1994. Sr-Nd isotope and trace-element geochemistry of late Variscan volcanism in the Pyrenees: magmatism in post-orogenic extension? Tectonophysics 238 (1–4), 161–181. https://doi.org/10.1016/0040-1951(94)90054-X.
Izart, A., the 343 IGCP working group, 1998. Stratigraphic correlations between the continental and marine Tethyan and Peri-Tethyan basins during the late Carboniferous and the early Permian. In: Crasquin-Soleau, S., Izart, A., Vaslet, D., De Wever, P. (Eds.), Peri-Tethys: Stratigraphic Correlations 2, Geodiversitas, vol. 20, pp. 521–595.
Izart, A., Stephenson, R., Vai, G.B., Vachard, D., Le Nindre, Y., Vaslet, D., Fauvel, P.-J., Suss, P., Kossovaya, O., Chen, Z., Maslo, A., Stovba, S., 2003. Sequence stratigraphy and correlation of late Carboniferous and Permian in the CIS, Europe, Tethyan area, North Africa, Arabia, China, Gondwanaland and the USA. Palaeogeogr. Palaeoclimatol. Palaeoecol. 196, 59–84.
Jabaloy, A., Galindo-Zaldívar, J., González-Lodeiro, F., 2002. Paleostress evolution of the Iberian Peninsula (Late Carboniferous to present-day). Tectonophysics 357, 159–186. https://doi.org/10.1016/S0040-1951(02)00367-0.

Jolivet, M., Labaume, P., Monié, P., Brunel, M., Arnaud, N., Campani, M., 2007. Thermochronology constraints for the propagation sequence of the south Pyrenean basement thrust system (France-Spain). Tectonics 26 (5). TC5007.
Julivert, M., 1971. Decollement tectonics in the Hercynian Cordillera of Northwest Spain. Am. J. Sci. 270 (1), 1–29.
Julivert, M., Marcos, A., 1973. Superimposed folding under flexural conditions in the Cantabrian Zone (Hercynian Cordillera, Northwest Spain). Am. J. Sci. 273 (5), 353–375.
Juncal, M.A., Diez, J.B., Broutin, J., Martínez-García, E., 2016. Palynolflora from the Permian Sotres Formation (Picos de Europa, Asturias, Northern Spain). Spanish J. Paleontol. 31, 85–94.
Juncal, M.A., Lloret, J., Diez, J.B., López-Gómez, J., Ronchi, A., De la Horra, R., Barrenechea, J.F., Arche, A., 2019. New Upper Carboniferous palynofloras from Southern Pyrenees (NE Spain): implications for palynological zonation of Western Europe. Palaeogeogr. Palaeoclimatol. Palaeoecol. 516, 307–321. https://doi.org/10.1016/j.palaeo.2018.12.010.
Lago, M., Arranz, E., Pocoví, A., Galé, C., Gil-Imaz, A., 2004a. Permian magmatism and basin dynamics in the Southern Pyrenees: A record of transition from late Variscan transtension to early Alpine extension. In: Wilson, M., Neumann, E.R., Davies, G.R., Timmerman, M.J., Heeremans, M., Larsen, B.T. (Eds.), Permo-Carboniferous Magmatism and Rifting in Europe, Geological Society, London, Special Publications, vol. 223, pp. 439–464.
Lago, M., Arranz, E., Pocoví, A., Galé, C., Gil-Imaz, A., 2004b. Lower Permian magmatism of the Iberian Chain, Central Spain, and its relationship to extensional tectonics. In: Wilson, M., Neumann, E.R., Davies, G.R., Timmerman, M.J., Heeremans, M., Larsen, B.T. (Eds.), Permo-Carboniferous Magmatism and Rifting in Europe, Geological Society, London, Special Publications, vol. 223, pp. 440–465.
Lago, M., Galé, C., Ubide, T., 2019. Permian and Triassic Magmatism in the Iberian Basin. In: Quesada, C., Oliveira, J. (Eds.), The Geology of Iberia: A Geodynamic Approach. Volume 3: the Alpine Cycle. Regional Geology Reviews. Springer, Heidelberg, pp. 79–81.
Lepvrier, C., Martínez-García, E., 1990. Fault development and stress evolution evolution of the post-Hercynian Asturian Basin (Asturias and Cantabria, northwestern Spain). Tectonophysics 184, 345–356.
Liesa, C.L., Soria, A.R., Meléndez, A., 2000. Lacustrine evolution in a basin controlled by extensional faults: The Galve subbasin, Teruel, Spain. In: Gierlowski-Kordesch, E.H. (Ed.), Lake Basins through Space and Time, American Association of Petroleum Geologists, Studies in Geology, vol. 46, pp. 295–302.
Lloret, J., 2019. Stratigraphic-Sedimentary Reconstruction in the Permian- Triassic Succession of the Central-Eastern Southern Pyrenees: A Multi-Disciplinary Approach. Università degli Studi di Pavia, Pavia, Italy. Ph.D. Unpublished.
Lloret, J., Juncal, M., 2018. Primeros datos palinológicos del Carbonífero superior en el Pirineo Oriental (Argestues, Lleida, España). Geogaceta 64, 91–94.
Lloret, J., Ronchi, A., López-Gómez, J., Gretter, N., De la Horra, R., Barrenechea, J.F., Arche, A., 2018. Syn-tectonic sedimentary evolution of the continental late Palaeozoic-early Mesozoic Erill Castell-Estac basin and its significance in the development of the central Pyrenees Basin. Sediment. Geol. 374, 134–157.
Lloret, J., De la Horra, R., Gretter, N., Borruel-Abadía, V., Barrenechea, J.F., Ronchi, A., Diez, J.B., Arche, A., López-Gómez, J., 2020. Gradual changes in the Olenekian-Anisian continental record and biotic implications in the Central-Eastern Pyrenean basin, NE Spain. Glob. Planet. Chang. 192, 103252. https://doi.org/10.1016/j.gloplacha.2020.103252.
Lloret, J., De la Horra, R., López-Gómez, J., Barrenechea, J.F., Gretter, N., Ronchi, A., 2021. Permian and Triassic paleosols in the fluvial- lacustrine record of the Central Pyrenees Basin, Spain: a stratigraphic tool for interpreting syn- tectonic sedimentary evolution and paleoclimate. Newsl. Stratigr. 54 (3), 377–404.
López-Gómez, J., Arche, A., Pérez-López, A., 2002. Permian and Triassic. In: Gibbons, W., Moreno, T. (Eds.), The Geology of Spain. The Geological Society, London, pp. 185–212.
López-Gómez, J., Martín-González, F., Heredia, N., De la Horra, R., Barrenechea, J.F., Cadenas, P., Juncal, M., Diez, J.B., Borruel-Abadia, V., Pedreira, D., García-Sansegundo, J., Farias, P., Galé, C., Lago, M., Ubide, T., Fernández-Viejo, G., Gand, G., 2019a. New lithostratigraphy for the Cantabrian Mountains: a common tectonostratigraphic evolution for the onset of the Alpine cycle in the W Pyrenean realm, N Spain. Earth Sci. Rev. 188, 249–271.
López-Gómez, J., Alonso-Azcárate, J., Arche, A., Arribas, J., Barrenechea, J.F., Borruel-Abadía, V., 43 coauthors, 2019b. Permian-Triassic Rifting Stage. In: Quesada, C., Oliveira, J. (Eds.), The Geology of Iberia: A Geodynamic Approach. Volume 3: The Alpine Cycle. Regional Geology Reviews. Springer, Heidelberg, pp. 29–112.
López-Gómez, J., De la Horra, R., Barrenechea, J.F., Borruel-Abadía, V., Martín-Chivelet, J., Juncal, M., Martín-González, F., Heredia, F., Diez, J.B., Buatois, L.A., 2021. Early Permian during the Variscan Orogen Collapse in the equatorial realm: insights from the Cantabrian Mountains (N Iberia) into climatic and environmental changes. Int. J. Earth Sci. https://doi.org/10.1007/s00531-021-02020.
López-Sánchez, M.A., Marcos, A., Martínez, F.J., Iriondo, A., Llana-Fúnez, S., 2015. Setting new constrains on the age of crustal-scale extensional shear zone (Vivero fault): implications for the evolution of Variscan orogeny in the Iberian massif. Int. J. Earth Sci. 104, 927–962.
López-Sánchez, M.A., García-Sansegundo, J., Martínez, F.J., 2019. The significance of early Permian and early Carboniferous U-Pb zircon ages in the Bossost and Lys-Caillaouas granitoids (Pyrenean Axial Zone). Geol. J. 54 (4), 2048–2063.
Lützner, H., Tichomirowa, M., KäBner, A., Gaupp, R., 2020. Latest Carboniferous to early Permian volcano-stratigraphic evolution in Central Europe: U–Pb CA–ID–TIMS ages of volcanic rocks in the Thuringian Forest Basin (Germany). Int. J. Earth Sci. 110, 377–398.
Maino, M., Dallagiovanna, G., Gaggero, L., Seno, S., Tiepolo, M., 2012. U–Pb zircon geochronological and petrographic constraints on late to post-collisional Variscan magmatism and metamorphism in the Ligurian Alps, Italy. Geol. J. 47 (6), 632–652.
Majoor, F.J.M., 1988. A Geochronological Study of the Axial Zone of the Central Pyrenees, with Emphasis on Variscan Events and Alpine Resetting. Ph.D. Thesis. Rijksuniversiteit Utrecht, Netherlands, 117p.
Manjón, M., Gutiérrez Claverol, M., Martínez-García, E., 1992. La sucesión posthercínica-preliásica del área de Villabona (Asturias, NW de España). In: III Congreso Geológico de España, Salamanca. Abstracts Book, 2, pp. 107–111.
Marcos, A., 1973. Las series del Paleozoico Inferior y la estructura herciniana del Occidente de Asturias (NW de España). Trab. Geol. 6, 3–113.
Martín-Chivelet, J., Berástegui, X., Rosales, I., 25 co-authors, 2002. Cretaceous. In: Gibbons, W., Moreno, T. (Eds.), The Geology of Spain. The Geological Society, London, pp. 255–292.
Martín-Chivelet, J., López-Gómez, J., Aguado, R., 43 co-authors, 2019. The Late Jrassic-Early Cretaceous Rifting. In: Quesada, C., Oliveira, J. (Eds.), The Geology of Iberia: A Geodynamic Approach. Volume 3: The Alpine Cycle. Regional Geology Reviews. Springer, Heidelberg, pp. 169–249.
Martínez Catalán, J.R., Rubio Pascual, F.J., Montes, A.D., Fernández, R.D., Barreiro, J.G., Dias Da Silva, Í., Clavijo, E.G., Ayarza, P., Alcock, J.E., 2014. The late Variscan HT/LP metamorphic event in NW and Central Iberia: relationships to crustal thickening, extension, orocline development and crustal evolution. Geol. Soc. Lond., Spec. Publ. 405, 225–247. https://doi.org/10.1144/sp405.1.
Martínez-Catalán, J.R., 2011. Are the oroclines of the Variscan belt related to late Variscan strike-slip tectonics? Terra Nova 23, 241–247.
Martínez-García, E., 1981. El Paleozoico de la Zona Cantábrica oriental. Trab. Geol. 11, 95–127.
Martínez-García, E., 1991a. Orogénesis y Sedimentación a Finales del Paleozoico en el NE del Macizo Ibérico (Asturias, Cantabria, Palencia). Vol. Homenaje A J. Ramírez del Pozo, A.G.G.E.P, pp. 167–174.
Martínez-García, E., 1991b. Hercynian syn-orogenic and post-orogenic successions in the in the Cambrian and Palentian zones (NW Spain). Comparison with other western European occurrences. Giorn. Geol. 53 (1), 208–228.
Martínez-García, E., 2004. El Pérmico de Asturias. In: Vera, J.A. (Ed.), Geología de España. SGE-IGME, pp. 268–269.
Martínez-García, E., Coquel, R., Gutiérrez Claverol, M., Quiroga, J.L., 1998. Edad del "tramo de transición" entre el Pérmico y el Jurásico en el área de Gijón (Asturias NW de España). Geogaceta 24, 215–218.
Martín-González, F., Heredia, N., 2011a. Geometry, structures and evolution of the western termination of the Alpine-Pyrenean Orogen reliefs (NW Iberian Peninsula). J. Iber. Geol. 37 (2), 103–120.
Martín-González, F., Heredia, N., 2011b. Complex tectonic and tectonostratigraphic evolution of an Alpine foreland basin: the western Duero Basin and the related Tertiary depressions of the NW Iberian Peninsula. Tectonophysics 502, 75–89.
Martín-González, F., Barbero, L., Capote, R., Heredia, N., Gallastegui, G., 2012. Interaction of two successive Alpine deformation fronts: constraints from low-temperature thermochronology and structural mapping (NW Iberian Peninsula). Int. J. Earth Sci. 101, 1331–1342.
Martín-González, F., Freudenthal, M., Heredia, N., Martín-Suárez, E., Rodríguez-Fernández, R., 2014. Palaeontological age and correlations of the Tertiary deposits of the NW Iberian Peninsula: the tectonic evolution of a broken foreland basin. Geol. J. 49 (1), 15–27.
Martín-González, F., Fernández-Lozano, J., De Vicente, G., Crespo-Martín, C., Heredia, N., 2021. Role of multiple inherited basement structures on orogen geometry and evolution: Insights from analogue modelling. J. Struct. Geol. 144, 104267. https://doi.org/10.1016/j.jsg.2020.104267.
Matte, P., 1986. La chaine varisque parmi les chaines paleozoiques peri-atlantiques, modèle d'evolution et position des blocs continentaux au Permo-Carbonifère. Bull. Soc. Geol. Fr. 8, 9–24.
McCann, T., Pascal, C., Timmerman, M., Krzywiec, P., López-Gómez, J., Wetzel, A., Krawczyk, C.M., Rieke, H., Lamarche, J., 2006. Post-Variscan (end Carboniferous – Early Permian) basin evolution in Western and Central Europe. In: Gee, D.G., Stephenson, R.A. (Eds.), European Lithosphere Dynamics. Geological Society London Memoirs, 32 (1), pp. 355–388.
Merino-Tomé, O., Bahamonde, J.R., Colmenero, J.R., Heredia, N., Villa, E., Farias, P., 2009. Emplacement of the Cuera and Picos de Europa imbricate system at the core of the Ibero-Armorican arc (Cantabrian Zone, N Spain): new precisions concerning the timing of arc closure. Geol. Soc. Am. Bull. 121, 729–751.
Merino-Tomé, O., Gutiérrez-Alonso, G., Villa, E., Fernández-Suárez, J., Martín Llaneza, J., Hofmann, M., 2017. LA-ICP-MS U-Pb dating of Carboniferous ash layers in the Cantabrian Zone (N Spain): stratigraphic implications. J. Geol. Soc. Lond. 174, 836–849.
Mey, P.H.W., Nagtegaal, P.J.C., Roberti, K.J., Hartevelt, J.J.A., 1968. Lithostratigraphic subdivision of post-Hercynian deposits in the South-Central Pyrenees, Spain. Leidse. Geol. Meded. 41, 221–228.
Miall, A.D., 1996. The Geology of Fluvial Deposits. In: Sedimentary Facies, Basin Analisis and Petroleum Geology. Springer, Berlin, 582 p.
Miall, A.D., 2014. Fluvial Depositional Systems. Springer, Berlin, 316 p.
Michel, L.A., Tabor, N.J., Montañeez, I.P., Schmitz, M.D., Davydov, V.I., 2015. Chronostratigraphy and Paleoclimatology of the Lodeve Basin, France: evidence for apan-tropical aridification event across the Carboniferous–Permian boundary. Palaeogeogr. Palaeoclimatol. Palaeoecol. 430, 118–131.
Mirouse, R., 1959. Extension et relation des séries permiennes sur la feuille d'Urdos au 80.000éme. Bulletin du Service de la Carte Géologique de la France 56 (257), 209–218.

Mirouse, R., 1966. Recherches géologiques dans la partie occidentale de la zone primaire axiale des Pyrénées. In: Mémoires Pour Servir a L'explication de la Carte Géologique Détaillée de la France, 451 p.
Montañez, I.P., Poulsen, C.J., 2013. The Late Paleozoic Ice Age: an evolving paradigm. Annu. Rev. Earth Planet. Sci. 41, 629–656.
Montañez, I.P., McElwain, J.C., Poulsen, C.J., White, J.D., Dimichele, W.A., Wilson, J.P., Griggs, G., Hren, M.T., 2016. Climate pCO2 and terrestrial carbon cycle linkages during late Palaeozoic glacial-interglacial cycles. Nat. Geosci. 9, 824–831.
Mujal, E., Fortuny, J., Oms, O., Bolet, A., Galobart, À., Anadón, P., 2016a. Palaeoenvironmental reconstruction and early Permian ichnoassemblage from the NE Iberian Peninsula (Pyrenean Basin). Geol. Mag. 153, 578–600.
Mujal, E., Gretter, N., Ronchi, A., López-Gómez, J., Falconnet, J., Díez, J.B., De la Horra, R., Bolet, A., Oms, O., Arche, A., Barrenechea, J.F., Steyer, J.S., Fortuny, J., 2016b. Constraining the Permian/Triassic transition in continental environments: stratigraphic and paleontological record from the Catalan Pyrenees (NE Iberian Peninsula). Palaeogeogr. Palaeoclimatol. Palaeoecol. 445, 18–37.
Mujal, E., Fortuny, J., Marmi, J., Dinarès-Turell, J., Bolet, A., Oms, O., 2018. Aridification across the Carboniferous-Permian transition in central equatorial Pangea: the Catalan Pyrenees succession (NE Iberian Peninsula). Sediment. Geol. 363, 48–68.
Muller, D., 1969. Perm und Trias im valle del Baztan (Spanische-Westpyrenäen). Dissertation, Fac. Natur.- Geisteswiss. T.U. Clausthal, 128 s., zahlr. Abb., Profilaf. U. 2 geol. Karten, Clausthal- Zellerfeld, 129 p.
Muñoz, J.A., 1992. Evolution of a continental collision belt: ECORS-Pyrenees crustal balanced section. In: McClay, K.R. (Ed.), Thrust Tectonics. Chapman and Hall, London, pp. 235–246.
Muñoz, J.A., 2002. Alpine tectonics I: The Alpine system north of the Betc Cordillera. Tectonic stting; the Pyrenees. In: Gibbons, W., Moreno, T. (Eds.), The Geology of Spain. Geological Society, London, pp. 370–385.
Muñoz, J.A., 2019. Alpine Orogeny: Deformation and Structure in the Northern Iberia Mrgin. In: Quesada, C., Oliveira, J. (Eds.), The Geology of Iberia: A Geodynamic Approach. Volume 3: The Alpine Cycle. Regional Geology Reviews. Springer, Heidelberg, pp. 433–447.
Murphy, D.H., Wilkinson, B.H., 1980. Carbonate deposition and facies distribution in a Central Michigan marl lake. Sedimentology 27, 123–135.
Muttoni, G., Gaetani, M., Kent, D.V., Sciunnach, D., Angiolini, L., Berra, F., Garzanti, E., Mattei, M., Zanchi, A., 2009. Opening of the Neo- Tethys Ocean, and the Pangaea B to Pangaea a transformation during the Permian. GeoArabia 14 (4), 17–48.
Nagtegaal, P.J.G., 1969. Sedimentology, palaeoclimatology and diagenesis of post-hercynian deposits in Southern-Central Pyrenees (Spain). Leidse. Geol. Meded. 42, 143–238.
Pedreira, D., Pulgar, J.A., Gallart, J., Torne, M., 2007. Three-dimensional gravity andmagnetic modeling of crustal indentation and wedging in the western Pyrenees-Cantabrian Mountains. J. Geophys. Res. 112. B12405.
Pereira, M.F., Castro, A., Chichorro, M., Fernández, C., Díaz-Alvarado, J., Martí, J., Rodríguez, C., 2014. Chronological link between deep-seated processes in magma chambers and eruptions: Permo-Carboniferous magmatism in the core of Pangaea (Southern Pyrenees). Gondwana Res. 25, 290–308.
Pérez-Estaún, A., Bastida, F., Alonso, J.L., Marquínez, J., Aller, J., Alvarez-Marrón, J., Marcos, A., Pulgar, J.A., 1988. A thin-skinned tectonic model for an arcuate fold and thrust belt: Cantabrian zone. Tectonics 7 (3), 517–537.
Pérez-Estaún, A., Martínez-Catalán, J.R., Bastida, F., 1991. Crustal thickenning and deformation sequence in the footwall to the suture of the Variscan belt of Northwest Spain. Tectonophysics 191, 243–253.
Platt, N.H., Wright, V.P., 1991. Lacustrine carbonates: Facies models, facies distributions and hydrocarbon aspects. In: Lacustrine facies analysis. In: Anadon, P., Cabrera, L., Kelts, K. (Eds.), Lacustrine Facies Analysis, Spec. Publ. Inter. Ass. Sediment, vol. 13, pp. 57–74.
Pulgar, J.A., Gallart, J., Fernández-Viejo, G., Pérez-Estaún, A., Álvarez-Viejo, J., 1996. Seismic image of the Cantabrian Mountains in the western extensión of the Pyrenees from integrated ESCIN reflection and refraction data. Tectonophysics 264, 1–19.
Pulgar, J.A., Alonso, J.L., Espina, R.G., Marín, J.A., 1999. La deformación alpina en el basamento varisco de la Zona Cantábrica. Trab. Geol. 21, 283–294.
Ramos, V., Folguera, A., 2009. Andean flat-slab subduction through time. In: Murphy, J. B., Keppie, J.D., Hynes, A.J. (Eds.), Ancient Orogens and Modern Analogues, Geological Society, London, Special Publications, vol. 327, pp. 31–54.
Ríos, L.M., Galera, J.M., Barettino, D., 1987. Hoja del Mapa Geológico de España a Escala 1:50.000 n° 145 (Sallent). Segunda Serie MAGNA-Primera Edición. Instituto Geológico y Minero de España, Madrid.
Robles, S., Llompart, C., 1987. Análisis paleogeográfico y consideraciones paleoicnológicas del Pérmico Superior y Triásico Inferior en la transversal del río Segre (Alt Urgell, Pirineo de Lérida). Cuadernos de Geología Ibérica 11, 115–130.
Robles, S., Quesada, S., Rosales, I., Aurell, M., García-Ramos, J.C., 2004. El Jurásico marino de la Cordillera Cantábrica. In: Gibbons, W., Moreno, T. (Eds.), Geology of Spain. The Geological Society, London, pp. 279–285.
Rodríguez-Fernández, L.R., Heredia, N., 1987. La estratigrafía del Carbonífero y la estructura de la Unidad del Pisuerga-Carrión. Cuadernos Laboratorio Xeolóxico Laxe 12, 207–229.
Rodríguez-Fernández, L.R., Heredia, N., 1988. Evolución tectonosedimentaria de una cuenca de antepaís ligada a una cadena arqueada: El ejemplo de la Unidad del Pisuerga-Carrión (Zona Cantábrica, NO de España). In: Libro Simposios, II Congreso Geológico de España, Granada. Simposio Cinturones Orogénicos, pp. 65–74.
Rodríguez-Méndez, L., Cuevas, J., Esteban, J.J., Tubía, J.M., Sergeev, S., Larionov, A., 2014. Age of the magmatism related to the inverted Stephanian–Permian basin of the Sallent area (Pyrenees). Geol. Soc. Lond. 394, 101–111.
Rodríguez-Méndez, L., Cuevas, J., Tubía, J.M., 2016. Post-Variscan basin evolution in the Central Pyrenees: insights from the Stephanian-Permian Anayet Basin. Compt. Rendus Geosci. 348 (3–4), 333–341.
Romer, R.L., Soler, A., 1995. U-Pb age and lead isotopic characterization of Au-bearing skarn related to the Andorra Granite (Central Pyrenees, Spain). Mineral. Deposita 30 (5), 374–383.
Saura, E., Teixell, A., 2006. Inversion of small basins: effects on structural variations at the leading edge of the Axial Zone antiformal stack (Southern Pyrenees, Spain). J. Struct. Geol. 28, 1909–1920.
Scotese, C.R., Langford, R.P., 1995. Pangea and the Paleogeography of the Permian. In: Cholle, P.A., Peryt, T.M., Ulmer-Scholle, D.S. (Eds.), The Permian of Northern Pangea. 1 Paleogeography, Paleoclim ates and Stratigraphy. Springer-Verlag, Berlin, pp. 1–19.
Simon, S.S.T., Gibling, M.R., 2017. Fine-grained meandering systems of the Lower Permian Clear Fork Formation of north-central Texas, AUA: lateral ans oblique accretion on an arid plain. Sedimentology 64, 714–746.
Sinclair, H.D., Gibson, M., Naylor, M., Morris, R.G., 2005. Asymmetric growth of the Pyrenees revealed through measurement and modeling of orogenic fluxes. Am. J. Sci. 305, 369–406.
Smith, G.A., 1987. Sedimentology of volcanism-induced aggradation in fluvial basins: Examples from the Pacific northwest, USA. In: Ethridge, F.G., Flores, R.M., Harvey, M.D. (Eds.), Recent Developments in Fluvial Sedimentology, Soc. Econ. Paleontol. Mineral. Spec. Publ, vol. 39, pp. 157–164.
Srivastava, S.P., Roest, W.R., Kovacs, L.C., Oakey, G., Le-Vesque, S., Verhoef, J., Macnab, R., 1990. Motion of Iberia since the Late Jurassic: results from detailed aeromagnetic measurement in the Newfoundland Basin. Tectonophysics 184, 229–260.
Stampfli, G.M., Borel, G.D., 2002. A plate tectonic model for the Paleozoic and Mesozoic constrained by dynamic plate boundaries and restored synthetic oceanic isochrons. Earth Planet. Sci. Lett. 196, 17–33.
Stolhofen, H., Stanistreet, I.G., 1994. Interaction between bimodal volcanism, fluvial sedimentation and basin development in the Permo-Carboniferous Saar-Nahe Basin (south-west Germany). Basin Res. 6 (4), 245–267.
Suárez, O., Cuesta, A., Gallastegui, C., Corretgé, L.G., 1993. Mineralogía y petrología de las tocas plutónicas de Infiesto (Zona Cantábrica, N de España). Trab. Geol. 19, 123–153.
Suárez, O., Gallastegui, G., Cuesta, A., Corretgé, L.G., 1999. Filiación geoquímica mantélica de las rocas ígneas de Salas-Belmonte: Implicaciones petrogenéticas (Zona Cantábrica, Macizo Ibérico). Trab. Geol. 21, 363–376.
Suárez-Rodríguez, A., 1988. Estructura del área de Villaviciosa-Libardón (Asturias, Cordillera Cantábrica). Trab. Geol. 17, 87–98.
Tabor, N.J., Montañez, I.P., 2004. Permo-Pennsylvanian alluvial paleosols (north-Central Texas): high-resolution proxy records of the evolution of early Pangean paleoclimate. Sedimentology 51, 851–884.
Teixell, A., 1998. Crustal structure and orogenic material budget in the west-Central Pyrenees. Tectonics 17, 395–406.
Teixell, A., García-Sansegundo, J., 1994. Hoja del Mapa Geológico de España a escala 1: 50.000 n° 118 (28-07) (Zuriza). In: Segunda serie MAGNA-Primera Edición. Instituto Geológico y Minero de España, Madrid.
Teixell, A., García-Sansegundo, J., Zamorano, M., 1994. Hoja del Mapa Geológico de España a escala 1: 50.000 n° 144 (28-08) (Ansó). In: Segunda serie MAGNA-Primera Edición. Instituto Geológico y Minero de España, Madrid.
Teixell, A., Labaume, P., Ayarza, P., Espurt, N., de Saint Blanquat, M., Lagabrielle, Y., 2018. Crustal structure and evolution of the Pyrenean-Cantabrian belt: a review and new interpretations from recent concepts and data. Tectonophysics 724, 146–170.
Ternet, Y., Majesté-Menjoulas, C., Canérot, J., Baudin, T., Cocherie, A., Guerrot, C., Rossi, P., 2004. Carte géologique de la France à 1: 50.000 n° 1069, Laruns-Somport et notice explicative de la feuille. In: Bureau de Recherches Géologiques et Minieres, Orleans.
Tugend, J., Manatschal, G., Kusznir, N.J., Masini, E., Mohn, G., Thinon, I., 2014. Formation and deformation of hyperextended rift systems: Insights from rift domain mapping in the Bay of Biscay-Pyrenees. Tectonics 33, 1239–1276.
Vacherat, A., Mouthereau, F., Pik, R., Bernet, M., Gautheron, C., Masini, E., LePourhiet, L., Tibari, B., Lahfid, A., 2014. Thermal imprint of rift-related processes in orogens as recorded in the Pyrenees. Earth Planet. Sci. Lett. 408, 296–306.
Vai, G.B., 2003. Development of the palaeogeography of Pangaea from Late Carboniferous to Early Permian. Palaeogeogr. Palaeoclimatol. Palaeoecol. 196, 125–155.
Valero-Garcés, B., Gisbert, J., 1992. Shallow carbonate lacustrine facies models in the Permian of the Aragón-Bearn basin (Western Spanish-French Pyrenees). Carbonates Evaporites 7 (2), 94–107.
Valero-Garcés, B., Gisbert, J., 2004. El Estephaniense y Pérmico de los Pirineos. In: Vera, J.A. (Ed.), Geología de España. SGE-IGME, Madrid, pp. 266–268.
Valverde-Vaquero, P., 1992. Permo-Carboniferous Magmatic Activity in the Cantabrian Zone (NE Iberian Massif, Asturias, NW Spain). MSc Thesis. Boston College, USA, 198p.
Valverde-Vaquero, P., Cuesta, A., Gallastegui, G., Suárez, O., Corretgé, L.G., Dunning, G., 1999. U-Pb dating of late variscan magmatism in the Cantabrian Zone (Northern Spain). J. Conf. Abstr. 4 (1). A04 4P/40.
Velando, F., Castelló, R., Orviz, F., Ortuño, G., Caride, C., Gervilla, M., Fernández-Pello, J., Obis, A., 1975. Memoria del Mapa Geológico de España E. 1:50.000 n° 53 (Mieres). In: Segunda Serie MAGNA-Primera Edición. IGME, 36 p.
Vergés, J., Burbank, D.W., 1996. Eocene-Oligocene thrusting and basin configuration in the Eastern and Central Pyrenees (Spain). In: Friend, P.F., Dabrio, C.J. (Eds.), Tertiary Basins of Spain. The Stratigraphic Record of Crustal Kinematics. Cambridge University Press. World and Regional Geology, pp. 120–133.

Vergès, J., García Senz, J., 2001. Mesozoic evolution and Cainozoic inversión of the Pyrenean Rift. In: Ziegler, P.A., Cavazza, W., Robertson, A.F.H., Crasquin-Soleau, S. (Eds.), Peri-Tethys Memoir 6: Peri-Tethyan Rift/Wrench Basins and Passive Margings, 186. Mémoires du Muséum national d'Histoire naturelle, pp. 187–212.

Voldman, G.G., Martínez-Chacón, M.L., Duffin, C.J., Fernández, L.P., Alonso, J.L., 2020. Pennsylvanian brachiopod, fish and conodont faunas from the Caliza Masiva (San Emiliano Formation) at the Mina Profunda area, Cantabrian Zone, NW Spain. Geobios 59, 91–106.

Wagner, R.H., Martínez-García, E., 1982. Description of an early Permian flora from Asturias and comments on similar occurrences in the Iberian Peninsula. Trab. Geol. 12, 273–287.

Williams, G.D., Fischer, M.W., 1984. A balanced section across the Pyrenean Orogenic Belt. Tectonics 3 (7), 773–780.

Williams, M.A.J., Assefa, G., Adamson, D.A., 1986. Depositional context of Plio-Pleistocene hominid-bearing formations in the Middle Awash valley, southern Afar Rift, Ethiopia. In: Frostick, L.E., Renaut, R.W., Reid, I., Tiercelin, J.-J. (Eds.), Sedimentation in the African Rifts, Geological Society Special Publication, vol. 25, pp. 241–251.

Wu, C., Ullah, M., Lu, J., Bhattacharya, J.P., 2016. Formation of point bars through rising and falling flood stages: evidence from bar morphology, sediment transport and bed shear stress. Sedimentology 63, 1458–1473.

Ziegler, P.A., 1990. Geological Atlas of Western and Central Europe. Shell internationale Petroleum Maastschappij BV. 2nd Edition. Geological Society Publishing House, Bath. International Lithosphere Program, 148, pp. 1–239.

Ziegler, P.A., 1993. Late Paleozoic-early Mesozoic plate reorganization: Evolution and demise of the Variscan fold belt. In: Ramer, J.F., Neubauer, F. (Eds.), Pre-Mesozoic Geology in the Alps. Springer Verlag, Berlin, pp. 203–216.

Ziegler, P.A., Stampfli, G.M., 2001. Late Paleozoic-early Mesozoic plate boundary reorganization: collapse of the Variscan orogen and opening of the Neotethys. Nat. Bresciana 27, 17–34.